Structural Distortions in *mer*-$M(H)_3(NO)L_2$ (M = Ru, Os) and Their Influence on Intramolecular Fluxionality and Quantum Exchange Coupling

Dmitry V. Yandulov, Dejian Huang, John C. Huffman, and Kenneth G. Caulton*,†

Department of Chemistry and Molecular Structure Center, Indiana University, Bloomington, Indiana 47405-4001

Received December 20, 1999

Molecules of the type *mer*-$M(H)_3(NO)L_2$ [M = Ru (**1**), Os (**2**); L = PR_3] are characterized on the basis of ^{1}H NMR T_{1min} values and IR spectra as pseudo-octahedral trihydrides significantly distorted by compression of the cis H−M−H angles to ∼75°. The distortion, uncharacteristic of six-coordinate d^6 complexes, is rationalized with DFT (B3LYP) calculations as being driven by increased H-to-M σ donation and by the exceptional π-accepting ability of linear NO^+. In both **1** and **2**, hydrides undergo intramolecular site exchange with $\Delta H_{HH}^{\ddagger}$(**1**) = 10−11 kcal/mol and $\Delta H_{HH}^{\ddagger}$(**2**) = 16−20 kcal/mol, depending on L, whereas for *mer*-$Ru(H)_3(NO)(P^tBu_2Me)_2$ (**1b**), moderate exchange couplings (up to 77 Hz) are featured in the low-temperature ^{1}H NMR spectra, in addition to chemical exchange. On the basis of experimental and theoretical results, a dihydrogen intermediate is suggested to mediate hydride site exchange in **1**. The cis H−M−H distortion shortens the tunneling path for the exchanging hydrides in **1**, thereby increasing the tunneling rate; diminishes the "conflict" between trans hydrides in the mer geometry; and decreases the nucleophilicity of the hydrides. The generality of the observed structural distortion and its dependence on the ligand environment in late transition metal tri- and dihydrides are discussed. A less reducing metal center is generally characterized by greater distortion.

Introduction

Structural distortions from octahedral geometry in d^n six-coordinate transition metal complexes are abundant for $n < 6$. Specifically considering complexes with strong σ donors, the numerous examples include complexes such as $[MMe_6]^q$ with d^0 (M = W, Nb^-, Ta^-), d^1 (M = Tc, Re), and d^2 (M = Ru, Os) metal centers[1−3] and d^4 $OsH_2Cl_2L_2$,[4] which prefer trigonal prism-derived geometries, whereas in d^0 *trans*,*trans*-$Ta(H)_2(L)X(OR)_2$,[5,6] d^2 $Cp^*Os(H)_5$,[7] d^4 *mer*,*trans*-$Os(H)_3XL_2$,[8] and d^4 *mer*,*trans*-$OsHCl_3L_2$[9] transoid hydrides (or phosphines in the latter case) strongly distort away from the trans geometry. The distortion in *mer*,*trans*-$Os(H)_3ClL_2$, in which two transoid hydrides symmetrically approach the third hydride to cis H−M−H angles of 60°, enables this six-coordinate complex to exhibit associative reactivity, such as coordination of Lewis bases[10] and hydrogenation of terminal acetylenes.[11] Additionally, the phenomenon of quantum mechanical exchange coupling in transition metal polyhydrides[12] has, to date, invariably been found to involve cisoid hydrides distorted toward each other such that ∠H−M−H is significantly less than 90°.

For ML_6 with a d^6 (low-spin) metal configuration, the octahedral geometry is the most stable, and significant distortions from it are very rarely found. Unless steric factors are involved, as in the case of $Fe(H)_2L_4$,[13] the known distortions are modest: in both $[CrH(CO)_5]^-$ and $MnH(CO)_5$, four equatorial carbonyls bend toward the apical hydride,[14] decreasing the ∠OC−M−H from 90° by 5.4° (Cr)[15] and by 7.2° (Mn).[16] Recently, however, Werner et al. structurally characterized $OsX(=CHR)Cl(CO)L_2$ complexes,[17] in which transoid phosphines L strongly distort[18] away from the carbene ligand toward ligand X, leading to L−Os−L angles of 167.5° (X = Cl) and 141.4° (X = H). The stability of the octahedral d^6 ML_6 structure makes nondissociative hydride fluxionality an infrequent occurrence,[13,19−22] and no d^6 ML_6 classical polyhydride is known to exhibit exchange coupling.[12]

Because of the strong hydride trans influence, the trans dihydride geometry is strongly destabilizing,[23,24] and stable trans dihydrides are relatively uncommon[13,25−32] compared to cis dihy-

† E-mail: caulton@indiana.edu.

(1) Kleinhenz, S.; Pfennig, V.; Seppelt, K. *Chem. Eur. J.* **1998**, *4*, 1687.
(2) Pfennig, V.; Seppelt, K. *Science* **1996**, *271*, 626.
(3) Kaupp, M. *Chem. Eur. J.* **1998**, *4*, 1678.
(4) Aracama, M.; Esteruelas, M. A.; Lahoz, F. J.; Lopez, J. A.; Meyer, U.; Oro, L. A.; Werner, H. *Inorg. Chem.* **1991**, *30*, 288.
(5) Parkin, B. C.; Clark, J. C.; Visciglio, V. M.; Fanwick, P. E.; Rothwell, I. P. *Organometallics* **1995**, *14*, 3002.
(6) Clark, J. R.; Pulvirenti, A. L.; Fanwick, P. E.; Sigalas, M.; Eisenstein, O.; Rothwell, I. P. *Inorg. Chem.* **1997**, *36*, 3623.
(7) Bayse, C. A.; Hall, M. B. *Inorg. Chim. Acta* **1997**, *259*, 179.
(8) Gusev, D. G.; Kuhlman, R.; Sini, G.; Eisenstein, O.; Caulton, K. G. *J. Am. Chem. Soc.* **1994**, *116*, 2685.
(9) Kuhlman, R.; Gusev, D. G.; Eremenko, I. L.; Berke, H.; Huffman, J. C.; Caulton, K. G. *J. Organomet. Chem.* **1997**, *536*, 139.
(10) Kuhlman, R.; Clot, E.; Leforestier, C.; Streib, W. E.; Eisenstein, O.; Caulton, K. G. *J. Am. Chem. Soc.* **1997**, *119*, 10153.
(11) Oliván, M.; Eisenstein, O.; Caulton, K. G. *Organometallics* **1997**, *16*, 2227.
(12) Sabo-Etienne, S.; Chaudret, B. *Chem. Rev.* **1998**, *98*, 2077.
(13) Meakin, P.; Guggenberger, L. J.; Jesson, J. P.; Gerlach, D. H.; Tebbe, F. N.; Peet, W. G.; Muetterties, E. L. *J. Am. Chem. Soc.* **1970**, *92*, 3482.
(14) Jackson, S. A.; Eisenstein, O.; Martin, J. D.; Albeniz, A. C.; Crabtree, R. H. *Organometallics* **1991**, *10*, 3062.
(15) Darensbourg, M.; Slater, S. *J. Am. Chem. Soc.* **1981**, *103*, 5914.
(16) La Placa, S. J.; Hamilton, W. C.; Ibers, J. A.; Davison, A. *Inorg. Chem.* **1969**, *8*, 1928.
(17) Werner, H.; Stüer, W.; Laubender, M.; Lehmann, C.; Herbst-Irmer, R. *Organometallics* **1997**, *16*, 2236.
(18) Gérard, H.; Clot, E.; Eisenstein, O. *New J. Chem.* **1999**, *23*, 495.
(19) Ball, G. E.; Mann, B. E. *J. Chem. Soc., Chem. Commun.* **1992**, 561.
(20) Bakhmutov, V.; Bürgi, T.; Burger, P.; Ruppli, U.; Berke, H. *Organometallics* **1994**, *13*, 4203.
(21) Bianchini, C.; Meali, C.; Peruzzini, M.; Zanobini, F. *J. Am. Chem. Soc.* **1987**, *109*, 5548.
(22) Heinekey, D. M.; van Roon, M. *J. Am. Chem. Soc.* **1996**, *118*, 12134.

10.1021/ic991452j CCC: $19.00
Published on Web 04/01/2000

Scheme 1

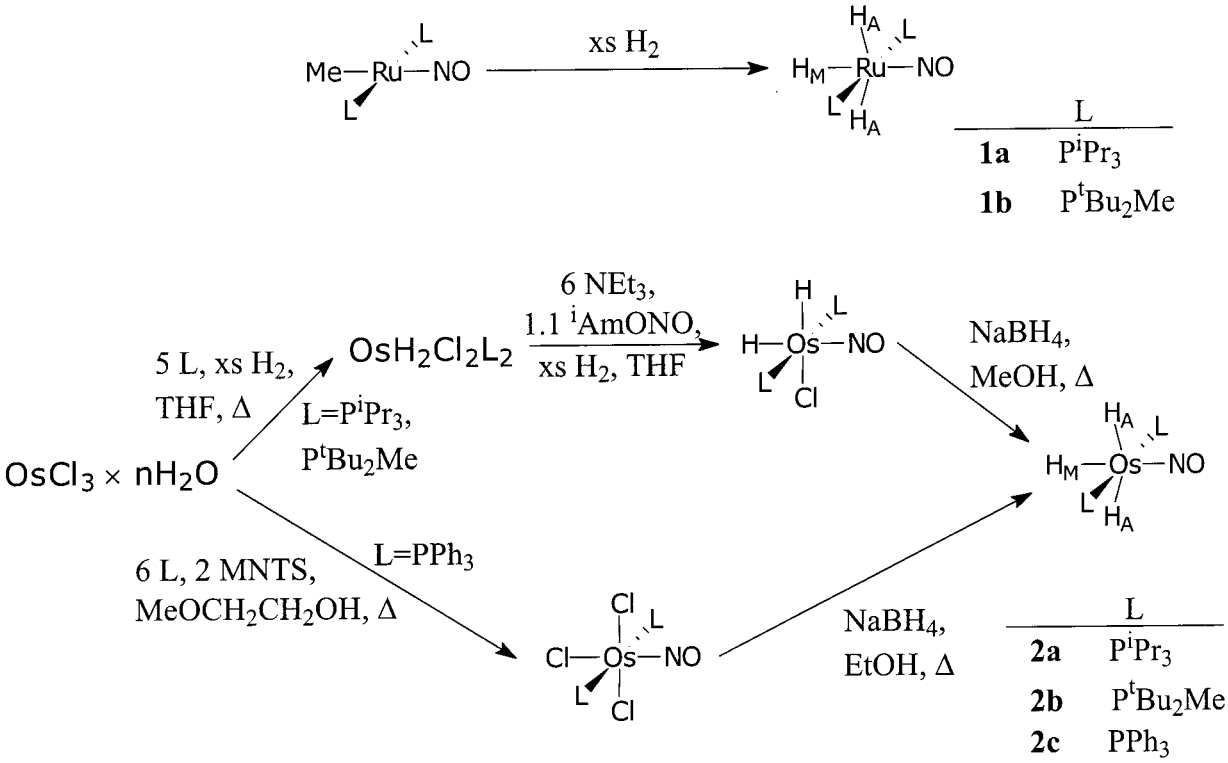

dride complexes. Although steric factors typically dictate the preference for the electronically unstable trans dihydride structure over the cis analogue,[33] both trans and cis isomers are often observed simultaneously in a detectable equilibrium.[13,27−29,31,32] An understanding of the factors stabilizing the trans dihydride geometry is desirable for rational control of hydride reactivity. For example, dihydrogen ligands in *trans*-$[M(X)(H_2)(P\sim P)_2]^+$ (M = Ru, Os) were computed[34] to be the least acidic with X = H out of an extensive series of ligands X, consistent with experimental results,[35] which implies a somewhat increased hydride nucleophilicity in the trans dihydride geometry.

Complexes of strongly reducing metal centers with strong π acids, in particular NO^+, are beginning to attract some attention, as very strong back-bonding interactions are anticipated to lead to unusual reactivity.[36] Such features of the electronic structure are primarily responsible for the "saw-horse" geometry adopted by d^8 $Ru(CO)_2L_2$[37,38] and $[Ru(CO)(NO)L_2]^+$ [39] with trans L, unusual for d^8 four-coordinate complexes. This work presents additional unusual consequences of strong back-bonding interactions with NO^+ on structure and reactivity. Despite having a formal d^6 metal configuration, *mer*,*trans*-$M(H)_3NOL_2$ (M = Ru, Os) compounds are significantly distorted from octahedral geometry by bending of the trans hydrides away from NO. The distortion stabilizes the transoid dihydride geometry and leads to observation of quantum mechanical exchange coupling in *mer*-$Ru(H)_3(NO)(P^tBu_2Me)_2$, the first d^6 pseudo-octahedral polyhydride to exhibit such a phenomenon.

Results

Synthesis. Ruthenium trihydrides $Ru(H)_3(NO)L_2$ [L = P^iPr_3 (**1a**), P^tBu_2Me (**1b**)] were prepared by hydrogenolysis of the corresponding *trans*-$Ru(Me)(NO)L_2$ complexes.[40] Because of their instability toward the H_2 loss, **1a**,**b** were generated in situ and studied under 1 atm of H_2.

Osmium trihydrides $Os(H)_3(NO)L_2$ [L = P^iPr_3 (**2a**), P^tBu_2Me (**2b**)] were synthesized via $NaBH_4$/MeOH reduction of the corresponding *cis*,*trans*-$OsH_2Cl(NO)L_2$ compounds[41,42] and isolated in high yield. The chloro precursors were prepared by a new one-pot synthesis, involving in situ generation of $OsH_2Cl_2L_2$[4] (Scheme 1). The latter instantaneously reacts with NEt_3, RNO (isoamyl nitrite or *N*-methyl-*N*-nitroso-*p*-toluenesulfonamide), and H_2 to quantitatively (NMR) yield $OsH_2Cl(NO)L_2$, isolated in high yield. The PPh_3 analogue **2c** has

(23) Lin, Z.; Hall, M. B. *J. Am. Chem. Soc.* **1992**, *114*, 6102.
(24) Lin, Z.; Hall, M. B. *Coord. Chem. Rev.* **1994**, *135*/*136*, 845.
(25) Immirzi, A.; Musco, A.; Carturan, G.; Belluco, U. *Inorg. Chim. Acta* **1975**, *12*, L23.
(26) Shaw, B. L.; Uttley, M. F. *J. Chem. Soc., Chem. Commun.* **1974**, 918.
(27) Paonessa, R. S.; Trogler, W. C. *J. Am. Chem. Soc.* **1982**, *104*, 1138.
(28) Jessop, P. G.; Rastar, G.; James, B. R. *Inorg. Chim. Acta* **1996**, *250*, 351.
(29) Brown, J. M.; Dayrit, F. M.; Lightowler, D. *J. Chem. Soc., Chem. Commun.* **1983**, 414.
(30) Fryzuk, M. D.; MacNeil, P. *Organometallics* **1983**, *2*, 682.
(31) Harrod, J. F.; Jorke, W. J. *Inorg. Chem.* **1981**, *20*, 1156.
(32) Gusev, D. G.; Lough, A. J.; Morris, R. H. *J. Am. Chem. Soc.* **1998**, *120*, 13138.
(33) For a notable exception, see: Rybtchinski, B.; Ben-David, Y.; Milstein, D. *Organometallics* **1997**, *16*, 3786.
(34) Xu, Z.; Bytheway, I.; Jia, G.; Lin, Z. *Organometallics* **1999**, *18*, 1761.
(35) Maltby, P. A.; Schlaf, M.; Steinbeck, M.; Lough, A. J.; Morris, R. H.; Klooster, W. T. *J. Am. Chem. Soc.* **1996**, *118*, 5396.
(36) Daff, J. P.; Legzdins, P.; Rettig, J. J. *J. Am. Chem. Soc.* **1998**, *120*, 2688.
(37) Ogasawara, M.; Macgregor, S. A.; Streib, W. E.; Folting, K.; Eisenstein, O.; Caulton, K. G. *J. Am. Chem. Soc.* **1995**, *117*, 8869.
(38) Ogasawara, M.; Macgregor, S. A.; Streib, W. E.; Folting, K.; Eisenstein, O.; Caulton, K. G. *J. Am. Chem. Soc.* **1996**, *118*, 10189.
(39) Ogasawara, M.; Huang, D.; Streib, W. E.; Huffman, J. C.; Gallego-Planas, N.; Maseras, F.; Eisenstein, O.; Caulton, K. G. *J. Am. Chem. Soc.* **1997**, *119*, 8642.
(40) Huang, D.; Streib, W. E.; Caulton, K. G. Manuscript in preparation.
(41) Werner, H.; Flügel, R.; Windmüller, B.; Michenfelder, A.; Wolf, J. *Organometallics* **1995**, *14*, 612.
(42) Yandulov, D. V.; Streib, W. E.; Caulton, K. G. *Inorg. Chim. Acta* **1998**, *280*, 125.

Table 1. Values for 300-MHz T_{1min} and Derived Structural Data[a] of *cis,trans*-$MH_2X(NO)L_2$ Compounds

			$[H]_n$[c]				$H[D]_{n-1}$[d]				
			T_{1min}, ms (T, °C)				T_{1min}, ms (T, °C)				
	$[M]X$[b]	L	H_M[h]	H_A[i]	r_{HH}, Å[e]	α_{HH}, deg[f]	H_M[h]	H_A[i]	r_{HH}, Å[e,j]	α_{HH}, deg[f,j]	avg.[g]
1a	$[Ru]H$[k]	P^iPr_3	140 (−105)	229 (−105)	1.9(1)	70(4)	304 (−105)	382 (−110)	1.99(7)	74(4)	**2.01(6)**
									2.0(1)	76(5)	**75(3)**
1b	$[Ru]H$[k]	P^tBu_2Me	141.9[j] (−100)	211.1[l] (−110)	**2.0(1)**	**73(5)**					
2a	$[Os]H$[m]	P^iPr_3	170.3 (−75)	281 (−75)	1.96(5)	71(3)	369 (−75)	458 (−75)	2.06(4)	76(3)	**2.09(4)**
									2.11(7)	78(4)	**77(3)**
2b	$[Os]H$[m]	P^tBu_2Me	181.3 (−80)	257 (−85)	2.1(1)	76(7)	412[n]	405[n]	2.07(7)	76(4)	**2.08(8)**
									2.1(1)	77(6)	**77(4)**
2c	$[Os]H$[o]	PPh_3	219 (−85)	381 (−85)	**2.01(5)**	**74(3)**					
	$[Os]Cl$[m]	P^iPr_3	201 (−60)	234 (−60)			311 (−60)	401 (−60)	2.02(8)	76(4)	**2.02(5)**
									2.02(6)	75(3)	**76(3)**

[a] Values in bold are the best estimates for each case (see Experimental Section for detailed discussion). [b] [M] = [*cis,trans*-$M(H)_2(NO)L_2$]. [c] All-protio isotopomers. [d] Partially deuterated isotopomers. [e] Distance between cis hydrides (errors) calculated from eq 1. [f] Angle between cis M−H bonds (errors). [g] Average H···H distances (errors) and angles (errors) from the two previous columns. [h] Hydride trans to NO. [i] Hydride(s) cis to NO. [j] Values calculated from H_M (first row) and H_A (second row) T_{1min} data according to eq 2. [k] In d_{10}-Et_2O. [l] Corrected for intramolecular $H_A \leftrightarrow H_M$ exchange. [m] In d_8-PhMe. [n] T_1 at T°C(T_{1min}) in the $(H)_3$ isotopomer. [o] In CD_2Cl_2.

recently been reported.[43] We employed an alternative two-step synthesis, as shown in Scheme 1.

Structure. (a) NMR. Solution NMR data unambiguously identify the C_{2v} *mer,trans*-$M(H)_3(NO)L_2$ geometries for **1** and **2**. In agreement with the data published[43] for **2c**, ^1H NMR spectra of **2a** and **2b** exhibit two high-field hydride signals as the A_2M part of the A_2MX_2 spin system (X = ^{31}P), that is, a triplet of doublets ($2H_A$) and a triplet of triplets (H_M) due to coupling with two ^{31}P nuclei and to coupling between H_A and H_M hydrides (Scheme 1). Phosphine alkyl signals show virtual coupling and do not exhibit diastereotopic inequivalence, as expected for a C_{2v}-symmetric structure with trans phosphines. The $^{31}P\{^1H\}$ signal is a singlet, which splits into a doublet of triplets upon selective decoupling of the alkyl resonances [$J(P-H_M) > J(P-H_A)$]. Ruthenium analogues **1a**,**b** show analogous spectra (in the absence of exchange, vide infra), except that the scalar $J(H_A-H_M)$ is not resolved at any observation temperature. All complexes exhibit strong ν(N−O) absorptions in solution IR spectra.

In contrast to **2a**,**b**, but in striking similarity to the isoelectronic $Ir(H)_3(CO)(PPh_3)_2$,[31,44] we find that $Os(H)_3(NO)(PPh_3)_2$ (**2c**) exists as a mixture of mer[45] and fac isomers, the latter persisting in solution at ∼5 mol %. Recent studies of a series of anionic transition metal polyhydrides[46,32] have shown how electrostatic and "dihydrogen" bonding interactions can serve to stabilize the *fac*-$[ML'](H)_3L_2$[q] (L′ = CO, NO, H; M = Re, Ru, Os, Ir) isomer over the mer analogue, forcing ligands as bulky as P^iPr_3 into cis positions. Although computationally we find a moderate electronic preference for *fac*-$M(H)_3(NO)(PH_3)_2$ over the mer isomer (vide infra), the former is only observed with our smallest ligand, PPh_3.

Originally, a DFT calculation showed that the pseudo-octahedral structure of the model *mer*-$Os(H)_3(NO)(PH_3)_2$ is significantly distorted by compression of the angles between the cis hydrides, $\angle H_A-Os-H_M$ (α_{HH}), to 72°. We sought to experimentally assess the extent of such "hydride bending" in compounds **1** and **2**, which is unusual for d^6 pseudo-octahedral complexes. The $H_A\cdots H_M$ distances (r_{HH}) were determined from the hydride T_{1min} values,[47] according to eqs[10,48] 1a and 1b.

$$\begin{cases} \dfrac{1}{T_{1min}(H_M)} = R_{1max}(H_M) = 2R_{1max}(H_A\cdots H_M) + R^*(H_M) \\ \dfrac{1}{T_{1min}(H_A)} = R_{1max}(H_A) = R_{1max}(H_A\cdots H_M) + R^*(H_A) \end{cases} \quad (1a)$$

$$\frac{1}{T_{1min}(H_M)} - \frac{1}{T_{1min}(H_A)} = R_{1max}(H_A\cdots H_M) = \frac{K_H}{r_{HH}^6} \quad (1b)$$

The dipolar relaxation contribution $R_{1max}(H_A\cdots H_M)$ is responsible for faster relaxation at the unique H_M site than that at H_A (Table 1), and it can be evaluated from eq 1a, assuming other relaxation mechanisms R^* are equal for both the H_A and the H_M sites, to yield the distance r_{HH} (Table 1) according to eq 1b (at 300 MHz, K_H = 129.21 Å^6 s^{-1}). Using T_{1min} values measured for the two hydride signals in $M(H_M)(H_A)_2(NO)L_2$ (**1a**, **2a**, and **2b**) and the corresponding $M(H)(D)_2(NO)L_2$ isotopomers, i.e., $M(H_M)(D_A)_2(NO)L_2$ and $M(D_M)(H_AD_A)(NO)L_2$, avoids the assumption $R^*(H_A) \approx R^*(H_M)$,[47] both of which are dominated by dipolar interactions with phosphine alkyl hydrogens, and gives two independent evaluations of r_{HH} (eqs 2a and 2b).

$$\begin{cases} \dfrac{1}{T_{1min}^{H_3}(H)_M} = 2R_{1max}(H_A\cdots H_M) + R^*(H_M) \\ \dfrac{1}{T_{1min}^{HD_2}(H)_M} = 2R_{1max}(D_A\cdots H_M) + R^*(H_M) \end{cases}$$

$$\begin{cases} \dfrac{1}{T_{1min}^{H_3}(H)_A} = R_{1max}(H_A\cdots H_M) + R^*(H_A) \\ \dfrac{1}{T_{1min}^{HD_2}(H)_A} = R_{1max}(D_A\cdots H_M) + R^*(H_A) \end{cases} \quad (2a)$$

$$\begin{cases} \dfrac{1}{T_{1min}^{H_3}(H)_M} - \dfrac{1}{T_{1min}^{HD_2}(H)_M} = 2\dfrac{K_H - K_D}{r_{HH}^6} \\ \dfrac{1}{T_{1min}^{H_3}(H)_A} - \dfrac{1}{T_{1min}^{HD_2}(H)_A} = \dfrac{K_H - K_D}{r_{HH}^6} \end{cases} \quad (2b)$$

The $R_{1max}(D_A\cdots H_M)$ term is the proton−deuteron dipolar relaxation contribution, evaluated under conditions of maximum $^1H-^1H$ relaxation (R^*)[47] and $K_H/K_D \approx 16$. The latter approach

(43) Clark, A. M.; Rickard, C. E. F.; Roper, W.; Wright, L. J. *J. Organomet. Chem.* **1997**, *543*, 111.
(44) Hasnip, S.; Duckett, S. B.; Taylor, D. R.; Taylor, M. J. *J. Chem. Soc., Chem. Commun.* **1998**, 923.
(45) The mer, trans isomer, unless otherwise stated.
(46) Abdur-Rashid, K.; Gusev, D. G.; Landau, S. E.; Lough, A. J.; Morris, R. H. *J. Am. Chem. Soc.* **1998**, *120*, 11826.

(47) See Supporting Information for a detailed discussion.

is more consistent and yields slightly greater r_{HH} distances, which correspond to upper estimates on the true values in the case of significantly anisotropic tumbling, as shown in the Supporting Information. Considering the corresponding experimental errors, the values derived using either approach (Table 1) are indistinguishable.

The metal−hydride distances, Os−H_M = 1.691 Å, Os−H_A = 1.670 Å, Ru−H_M = 1.650 Å, and Ru−H_A = 1.645 Å, were obtained from DFT calculations on the model *mer*-M(H)$_3$(NO)-(PH$_3$)$_2$ (vide infra). These values fall between the neutron diffraction ranges[49] for molecular and ternary terminal M−H bonds of 1.62−1.681 and 1.682−1.77 for Os and 1.599−1.630 and 1.665−1.792 for Ru. Of the characterized two ruthenium and three osmium molecular hydride complexes with terminal hydrides, none has a pseudo-octahedral geometry with strong trans-influencing ligands trans to the hydrides, for example, H and NO. Hence, the distances in ternary metal hydrides (such as octahedral $[MH_6]^{2-}$) should be considered as the upper limits on the true values in *mer*-M(H)$_3$(NO)L$_2$. Thus, the calculated M−H distances are quite reasonable estimates and were used with 0.05 Å errors in the derivation of α_{HH} from the r_{HH} values (Table 1).

All of the α_{HH} values shown in Table 1 are well below 90°, and for all of M(H)(D)$_2$(NO)L$_2$ complexes studied, the lower values derived from eq 2, not affected by variations in R^* between the H_A and H_M sites, are significantly different from 90° (in the 3σ sense) and are shown[47] to be the upper limits on the true values in the case of anisotropic tumbling. Thus, complexes **1** and **2** are subject to significant distortions from the pseudo-octahedral geometry by compression of the cis $\angle H_A-M-H_M$ angles. Within the experimental errors, all α_{HH} values are indistinguishable and cluster around 75°.

(b) DFT. DFT calculations (vide infra) largely support the experimental findings on the distorted structures of *mer*-M(H)$_3$-(NO)L$_2$ (M = Ru, Os). Using a moderate basis set (BS I) and PH_3 as the model phosphines, the values of α_{HH} in *mer*-M(H)$_3$-(NO)L$_2$ are 70.4° (Ru) and 72.3° (Os). Increasing the basis set to supplement the metal-bound atoms with polarization functions (BS II) or improving the model phosphines to PMe_3[50] increases the α_{HH} values by 1−2°, improving the agreement with experiment (Table 1), although the BS I/PH_3 values are qualitatively acceptable considering the experimental errors. The small magnitude of the calculated variations in α_{HH} on going from Ru to Os or on increasing the donor power of the phosphines (PMe_3 vs PH_3) makes it unlikely that such differences could be detected experimentally (Table 1).

(c) IR. Although our X-ray structure determination of Os-(H)$_3$(NO)(P^{i}Pr$_3$)$_2$ (**2a**, Supporting Information) was plagued by disorder and the hydrides were not located, additional evidence for hydride bending was obtained from solution IR spectra. The IR spectrum of **2a** in heptane (Figure 1) exhibits two weak bands in the region of M−H and N−O stretching frequencies, in addition to the very strong ν(N−O). The broad band at ∼2000 cm^{-1} has a shoulder on the high-frequency side and can be deconvoluted into two Gaussian lines (inset of Figure 1). Because deuteration of the hydride sites shifts all three high-frequency bands to lower frequencies (Figure 1), they correspond to Os−H stretching vibrations. All four bands can then be assigned to the specific Os−H and N−O stretching modes (Table 2) on the basis of qualitative agreement between observed and DFT-calculated [*mer*-Os(H)$_3$(NO)(PH$_3$)$_2$, BS I] frequencies

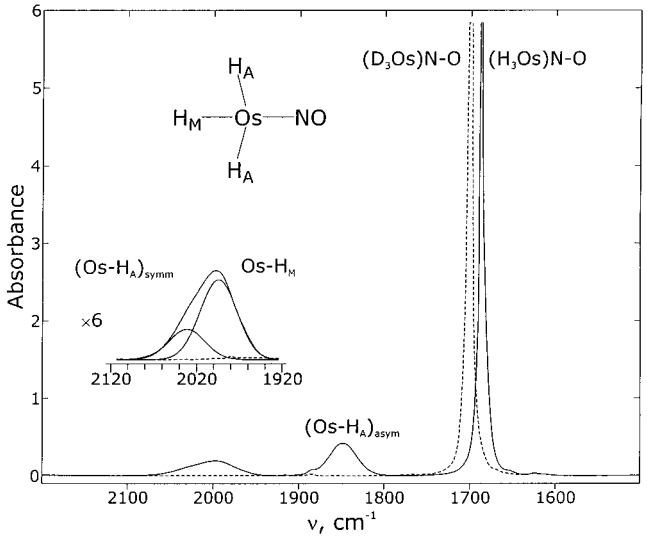

Figure 1. IR spectra [ν(Os−H) and ν(N−O) regions, *n*-heptane, 20 °C] of Os(H)$_3$(NO)(P^{i}Pr$_3$)$_2$ (**2a**, solid lines) and Os(D)$_3$(NO)(P^{i}Pr$_3$)$_2$ (>97 mol % D, dashed lines) with the solvent spectrum subtracted and bands assigned. The inset shows deconvolution of the broad asymmetric band at 2000 cm^{-1}.

Table 2. Observed and DFT-Calculated ν(Os−H) and ν(N−O) Frequencies and Intensities in *mer*-Os(H)$_3$(NO)(P^{i}Pr$_3$)$_2$ (**2a**)

	observed[a]		calculated[b]	
mode	ν, cm^{-1}	I^c, cm^{-1}	ν, cm^{-1}	I^d, km mol^{-1}
N−O[e]	1688	60.8	1673	539
(Os−H$_A$)$_{asym}$	1849	17.6	1940	110
Os−H$_M$[e]	1995	9.2	2001	92
(Os−H$_A$)$_{symm}$	2032	3.4	2059	27

[a] Measured in *n*-heptane at 20 °C. [b] *mer*-Os(H)$_3$(NO)(PH$_3$)$_2$, BS I, harmonic frequencies. [c] Integrated absorbance. [d] Integrated absorption intensity. [e] N−O and Os−H$_M$ modes are mixed.

and intensities. According to the textbook treatment of ν(C−O) intensities,[51] analogously applied to ν(M−H) intensities,[5] the ratio I(Os−H$_A$)$_{asym}$/I(Os−H$_A$)$_{symm}$ is tan^2 α_{HH}, from which an α_{HH} value of 66° can be derived. This result qualitatively supports the hydride bending phenomenon. The DFT-calculated intensities yield α_{HH} = 64°, in marked contrast to the actual value α_{HH} = 72.3°, which shows the qualitative nature of the treatment of IR intensities in our case,[52] even if very accurate experimental intensities are available.

Reactivity. (a) M = Os. The new Os(H)$_3$(NO)L$_2$ [L = P^{i}Pr$_3$ (**2a**), P^{t}Bu$_2$Me (**2b**)] complexes are quite robust. Both withstand harsh synthetic conditions (90 °C in MeOH for 14 h under H_2) and are moderately to not at all air- and moisture-sensitive. In contrast, **2c** (L = PPh_3) decomposes within minutes at 100 °C in toluene, producing observable quantities of OsH(NO)-(PPh_3)$_3$,[53] and has been proposed[43] to lose H_2 at elevated temperatures. Under ambient conditions, **2a** is inert to D_2 or CO (1 atm), and **2c** to D_2 (1 atm) or P^{i}Pr$_3$ (7 equiv), in benzene for 24 h. However, slight deuterium incorporation into hydride positions of **2a** occurs on prolonged heating at 90 °C in C_6D_6 or

(48) Castillo, A.; Esteruelas, M. A.; Oñate, E.; Ruiz, N. *J. Am. Chem. Soc.* **1997**, *119*, 9691.
(49) Bau, R.; Drabnis, M. H. *Inorg. Chim. Acta* **1997**, *259*, 27.
(50) Clot, E.; Eisenstein, O. *J. Phys. Chem. A* **1998**, *102*, 3592.
(51) Cotton, F. A.; Wilkinson, G. *Advanced Inorganic Chemistry*; John Wiley & Sons: New York, 1988; p 1035.
(52) At the B3LYP/BS I level, there is a slight coupling of the ν(Os−H$_M$) and ν(Os−H$_A$)$_{symm}$ modes, such that the intensity of the latter band in *mer*-Os(H)$_3$(NO)(PH$_3$)$_2$ is nearly twice as great as that of the corresponding band in *mer*-OsD$_M$(H$_A$)$_2$(NO)(PH$_3$)$_2$. Using the intensities calculated for the latter isotopomer gives α_{HH} = 70°, much closer to the actual value of α_{HH} = 72.3°.
(53) Osborn, J. A.; Wilson, S. T. *J. Am. Chem. Soc.* **1971**, *93*, 3068.

d_8-PhMe, accompanied by trace decomposition. These observations confirm that compounds **2** are saturated, although isotope exchange with arene solvents is consistent with phosphine loss as the energetically easiest access to an unsaturated intermediate, at least for **2a**,**b**.

Both **2a** and **2b** are inert to NpLi in benzene or THF for at least several hours, which characterizes the hydride ligands in these species at least as not acidic. Hydrides of **2a**,**b** show only negligible deuterium incorporation after 3 h at 90 °C in d_4-MeOH, comparable to that observed in C_6D_6, and the deuterated analogues of **2a** can be successfully recrystallized from h_4-MeOH without significant loss of D. The strong acids $[Ph_3C][BAr^F_4]$ and HOTf react with **2a**,**b** instantaneously, producing the known[42] $[Os(H)_2(NO)L_2]^+$ and $Os(H)_2(OTf)(NO)L_2$ species and the corresponding P^tBu_2Me analogues, although **2b** is inert to $Et_3N{\cdot}3HF$ at room temperature (RT) in benzene. Thus, hydrides in **2a**,**b** can be further characterized as moderately basic to neutral. Clean reactions between **2a** and solvents CD_2Cl_2 ($t_{1/2} \approx 24$ h) and $CDCl_3$ ($t_{1/2} \approx 20$ min), producing $Os(H)_2Cl(NO)L_2$, and CHD_2Cl, $CHDCl_2$, respectively, conceivably mediated by electron transfer, speak for some reducing character of the hydrides, consistent with their moderate basicity.

(b) M = Ru. Ruthenium trihydrides $Ru(H)_3(NO)L_2$ [L = P^iPr_3 (**1a**), P^tBu_2Me (**1b**)] easily lose H_2 (for example, under vacuum), producing the recently prepared[40] four-coordinate *trans*-$RuH(NO)L_2$. Under ambient conditions in solution under 1 atm of H_2, fast dynamic equilibrium (eq 3) is evident in the ^1H NMR spectra of **1**.

$$Ru(H)_3(NO)L_2 \underset{k_{-1}}{\overset{k_1}{\rightleftharpoons}} RuH(NO)L_2 + H_2 \qquad (3)$$

For **1b**, the free H_2 signal is not observed at 20 °C, but appears as an extremely broad peak at 0 °C, which progressively sharpens on further cooling. For **1a**, the rate of H_2 loss is significantly slower. With the similar $[H_2]/[\mathbf{1a}]$ and $[H_2]/[\mathbf{1b}]$ ratios, the free H_2 signal has a line width in the presence of **1a** at +20 °C in d_{10}-Et_2O similar to that of the signal with **1b** at −20 °C in d_8-PhMe. Quantitative H_2 line-width evaluations allow the rate constants for H_2 loss (k_1) to be determined,[54] which yield the corresponding $\Delta G^{\ddagger}_1$ values. Because of (possible) significant systematic errors in underestimating the relative H_2 concentration, these are reported as $\Delta G^{\ddagger}_1(\mathbf{1b},-20°C) \geq 12$ kcal/mol and $\Delta G^{\ddagger}_1(\mathbf{1a},+20°C) \geq 14$ kcal/mol.

The hydride signal of $RuH(NO)(P^iPr_3)_2$ in d_{10}-Et_2O (−9.98 ppm at 20 °C) shows no shift or broadening on cooling to −70 °C and is very close to that measured for $RuH(NO)(P^tBu_2Me)_2$ at 20 °C in C_6D_6 (9.28 ppm) or d_{14}-MeCy (9.30 ppm), suggesting that solvent coordination does not occur. X-ray structure determination of $RuMe(NO)(P^iPr_3)_2$ showed no sign of agostic interactions with phosphine alkyl groups.[40] Thus, to a good approximation, (a) the dynamic processes (eq 3) operating in d_{10}-Et_2O and d_8-PhMe are identical and (b) the forward reaction of eq 3 is a dissociative process [that is, the unsaturated $RuH(NO)L_2$ is not stabilized by either solvent coordination or agostic interaction], for which $\Delta S^{\ddagger}_1 \geq 0$ is expected.[55] The systematic errors in $\Delta G^{\ddagger}_1$ evaluations should largely cancel for the difference $\Delta G^{\ddagger}_1(\mathbf{1a},+20°C) - \Delta G^{\ddagger}_1(\mathbf{1b},-20°C)$, and therefore, with $\Delta S^{\ddagger}_1(\mathbf{1}) \geq 0$, the difference

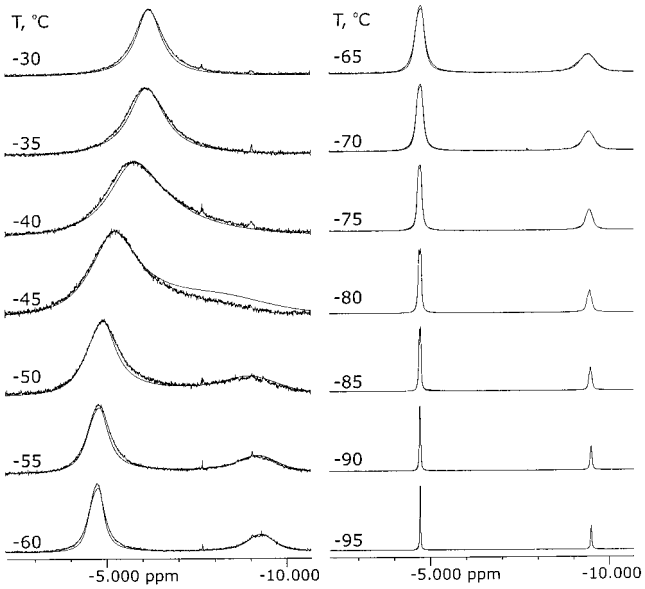

Figure 2. Superimposed calculated and observed (d_{10}-Et_2O, under 1 atm of H_2) variable-temperature 300-MHz $^1H\{^{31}P\}$ spectra of $Ru(H)_3(NO)(P^tBu_2Me)_2$ (**1b**).

$\Delta H^{\ddagger}_1(\mathbf{1a}) - \Delta H^{\ddagger}_1(\mathbf{1b})$ for H_2 loss can be estimated as ≥2 kcal/mol. Very similar results were obtained for the kinetics of H_2 loss[54] from $Os(H)_2(H_2)(CO)L_2$ [$\Delta G^{\ddagger}_1(P^iPr_3) - \Delta G^{\ddagger}_1(P^tBu_2Me) \approx 2$ kcal/mol], which, consistent with other thermochemical measurements,[56] indicate that $RuH(NO)(P^iPr_3)_2$ is more reducing toward H_2 than is the $RuH(NO)(P^tBu_2Me)_2$ analogue.

Because the T_{1min} values are measured for the hydride signals of **1** at very low temperatures (Table 1), the loss of H_2 does not influence the measurements or the reliability of the trihydride formulation $Ru(H)_3(NO)L_2$ as opposed to $RuH(H_2)(NO)L_2$. Furthermore, T_1 measurements for **1b** from 20 °C through T°C (T_{1min}) show no additional minimum or maximum at higher temperatures, providing no direct evidence for the existence of a second isomer. Such a temperature dependence would be expected if a nonclassical $RuH(H_2)(NO)L_2$ isomer was sufficiently *populated* and had a sufficiently *long lifetime* to cause partial T_1 averaging.[57]

Fluxionality. (a) M = Ru. In addition to exchange with free H_2, the six-coordinate $Ru(H)_3(NO)L_2$ complexes are subject to facile intramolecular hydride site exchange. At −30 °C in d_{10}-Et_2O, the ^1H NMR spectrum of **1b** exhibits a single broad hydride peak (site exchange with free H_2 has been essentially stopped), which broadens and decoalesces at −45 °C into two signals with a 2:1 intensity ratio ($2H_A$:$1H_M$) that progressively sharpen down to T°C(T_{1min}) (Figure 2). Oxidative addition of D_2 to $RuH(NO)L_2$ (L = P^iPr_3) in d_{10}-Et_2O at −100 °C shows (within 10 min) production of $RuH(D)_2(NO)L_2$ with H statistically scrambled among the H_A and H_M sites,[58] which persists for hours at low temperatures, rather than showing $Ru(D)_3(NO)L_2$ production, which supports the presence of intramolecular hydride site exchange. Additional evidence for the chemical exchange between H_A and H_M sites comes from averaging of the H_A and H_M hydride T_1 times, which, separately measured for **1b** at T°C ≤ −70, are partially exchange-averaged from −95 through −110 °C in d_{10}-Et_2O[59] (Figure 3). Assuming that

(54) Gusev, D. G.; Kuhlman, R. L.; Renkema, K. B.; Eisenstein, O.; Caulton, K. G. *Inorg. Chem.* **1996**, *35*, 6775.
(55) For example, 10 cal mol^{-1} K^{-1} for H_2 loss from $OsHCl(H_2)(CO)(P^iPr_3)_2$: Bakhmutov, V. I.; Bertrán, J.; Esteruelas, M. A.; Lledós, A.; Maseras, F.; Modrego, J.; Oro, L.; Sola, E. *Chem. Eur. J.* **1996**, *2*, 815.
(56) Li, C.; Ogasawara, M.; Nolan, S. P.; Caulton, K. G. *Organometallics* **1996**, *15*, 4900.
(57) Jessop, P. G.; Morris, R. H. *Coord. Chem. Rev.* **1992**, *121*, 155.
(58) The kinetic product was observed in the case of Os (vide infra).
(59) At T°C ≤ −95, $J(H_A-H_M) \leq 4.4$ Hz.

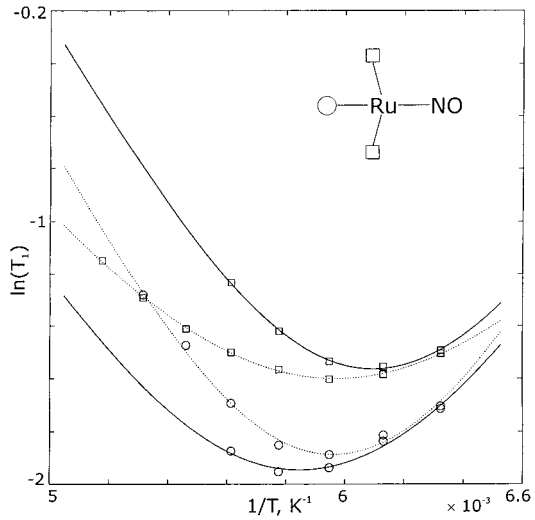

Figure 3. Observed (d_{10}-Et_2O, under 1 atm of H_2, dotted lines) and site-exchange-corrected (solid lines) T_1 times of the hydrides in $Ru(H)_3(NO)(P^tBu_2Me)_2$ (**1b**). Curves were fit to the $^1H-^1H$ dipolar relaxation mechanism (see Experimental Section).

Scheme 2

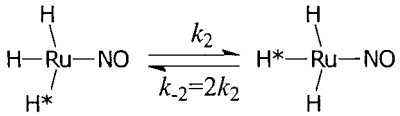

Table 3. Rate Constants for the Pairwise Hydride Site Exchange (k_{HH}) and H_A-H_M Coupling Constants (J_{HH})[a] for $Ru(H)_3(NO)(P^tBu_2Me)_2$ (**1b**) Obtained from Line-shape Analysis of the $^1H\{^{31}P\}$ Spectra in d_{10}-Et_2O under 1 atm of H_2

T, °C	J_{HH}, Hz	k_{HH}, s^{-1}	T, °C	J_{HH}, Hz	k_{HH}, s^{-1}
−30	400	7400	−65	47.8	160
−35	310	5300	−70	35.9	110
−40	237	3000	−75	24.0	56
−45	179	1700	−80	17.6	30
−50	134	800	−85	11.7	17
−55	99	490	−90	7.9	<10
−60	76.9	290	−95	4.4	<10

[a] Values from −95 through −60 °C were obtained by simultaneous fitting of k_{HH} and J_{HH}, extrapolated to higher temperatures according to an exponential law (see Experimental Section), and kept constant during simulations.

the observed intramolecular chemical exchange process is effected by pairwise hydride site exchange (Scheme 2), the spectra in Figure 2 were analyzed for kinetic parameters. The rate constants k_{HH} (=k_2), obtained from iterative line-shape fitting (Table 3, Figure 2), yield $\Delta H^{\ddagger}_{HH}$(**1b**) = 9.8(2) kcal/mol and $\Delta S^{\ddagger}_{HH}$(**1b**) = −0.4(11) cal mol^{-1} K^{-1} for the pairwise hydride site exchange from the Eyring plot (Figure 4). The essentially zero value of $\Delta S^{\ddagger}_{HH}$ is consistent with an intramolecular process, whereas the extrapolated value of $\Delta G^{\ddagger}_{HH}$(**1b**,−20°C) = 9.9(4) kcal/mol is distinctly lower than that for H_2 loss, namely, $\Delta G^{\ddagger}_1$(**1b**,−20°C) ≥ 12 kcal/mol.

Most notably, $^1H\{^{31}P\}$ NMR spectra of **1b** exhibit large and temperature-dependent H_A-H_M coupling, decreasing from 77 to 4.4 Hz as the temperature is lowered from −60 to −95 °C (Table 3, Figure 2).[60] Such a phenomenon is rather well-documented and understood in terms of quantum mechanical exchange.[12] Because, to the best of our knowledge,[12] no strictly

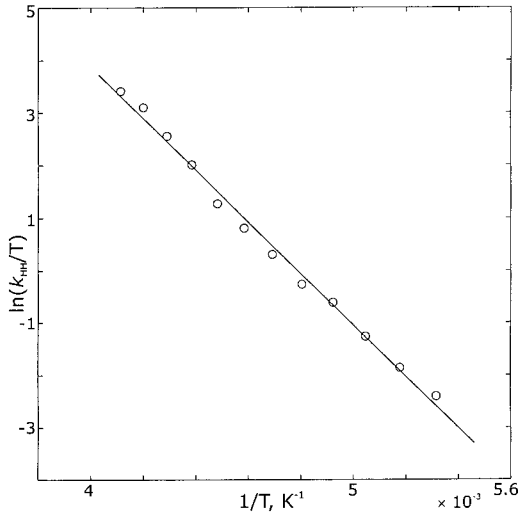

Figure 4. Eyring plot of the rate constants for the hydride site exchange in $Ru(H)_3(NO)(P^tBu_2Me)_2$ (**1b**).

octahedral transition metal cis polyhydride (with $\alpha_{HH} \approx 90°$) is known to exhibit exchange coupling, its existence for **1b** is consistent with the distorted structure of the complex, given a modest barrier for the hydride site exchange.

Compared to that in **1b**, the hydride site exchange in **1a** (L = P^iPr_3) is significantly slower, and moreover, ^1H NMR spectra (in d_{10}-Et_2O) exhibit no H_A-H_M coupling in the intermediate through stopped exchange regions (from −70 through −115 °C), with lines being ≥5 Hz ($W_{1/2}$) in width. Line-shape analysis yields k_{HH}(**1a**) = 130 (−55 °C) and 10 (−70 °C) s^{-1}, significantly lower than the corresponding values for **1b** (Table 3, 10% relative errors), which, with $\Delta S^{\ddagger}_{HH}$(**1a**) = $\Delta S^{\ddagger}_{HH}$(**1b**) ≈ 0, yield $\Delta H^{\ddagger}_{HH}$(**1a**) = 11 kcal/mol.[61] The higher barrier for chemical exchange, therefore, lowers the exchange coupling magnitude, as expected.[12] Furthermore, the fact that the parallel behavior of $\Delta H^{\ddagger}_{HH}$ for hydride site exchange with $\Delta H^{\ddagger}_1$ for H_2 loss can be experimentally detected provides strong support for the dihydrogen $[RuH(NO)L_2](H_2)$ transition state mediating the hydride site exchange. If the differences in $\Delta H^{\ddagger}_{HH}$ for **1a** and **1b** were to be due to the different steric requirements of P^iPr_3 and P^tBu_2Me, the latter was shown[56] to be slightly bulkier, so an exchange mechanism with a classical $[RuH(NO)L_2](H)_2$ transition state would only be easier for the smaller P^iPr_3, if a reduction in the P−Os−P angle were involved. It is also notable that $^1H\{^{31}P\}$ NMR spectra of **1b** exhibit no H_A-H_M coupling from −100 through −115 °C, with hydride signals broadening by <2 Hz. Together with analogous observations made for **1a**, the scalar $|J_{HH}|$ in **1** appears to be ≤3 Hz. This contrasts to $|J_{HH}|$ values of 5−6 Hz observed for all **2** and, among other factors, may be due to smaller α_{HH} in the case of ruthenium (vide supra).

(b) M = Os. All osmium derivatives, $Os(H)_3(NO)L_2$ (**2**), also undergo hydride site exchange in solution under ambient conditions, but with rates much slower than those measured for the ruthenium analogues **1a**,**b**. For L = P^iPr_3 (**2a**) and P^tBu_2Me (**2b**), no line-shape effects are evident by ^1H NMR at 20 °C, and only slight broadening of the hydride signals in **2a** is effected by raising the temperature to 80 °C in d_8-PhMe; the resonances retain all couplings. However, reactions between D_2 and independently prepared[62] transient $\{OsH(NO)L_2\}$ (L =

(60) Although fine structure is resolved only from −95 through −75 °C, spectra at −70 through −60 °C could be consistently reproduced by simultaneously optimizing both k_{HH} and J_{HH}.

(61) The ^1H NMR spectra of **1a** reveal no fine structure at T°C > −70 and may contain unresolved exchange couplings, which would result in an overestimation of k_{HH}(**1a**,−55°C).

P^iPr_3, P^tBu_2Me) after 15 min at RT cleanly produce $OsH(D)_2(NO)L_2$, with H statistically scrambled among the two H_A and H_M sites. Following this D_2 reaction for L = P^iPr_3 by ^1H NMR beginning at −40 °C in d_8-PhMe shows that, under the kinetic conditions, $Os(D_M)(H_AD_A)(NO)L_2$ is predominantly formed and that this species readily scrambles H as the temperature is raised to 20 °C. For L = PPh_3, the exchange is significantly faster, and ^1H NMR hydride signals of the major mer isomer are observably exchange-broadened already at 20 °C. Raising the temperature to 120 °C in d_8-PhMe leads to further broadening and a coalescence of the *mer*-**2c** hydride signals into a single broad peak, similar to the behavior observed for **1**. The signals of the minor *fac*-**2c** isomer, located within 0.5 ppm of the *mer*-**2c** H_A signal, also broaden and disappear at the *mer*-**2c** coalescence temperature, possibly because *fac*-**2c** is involved in the *mer*-**2c** hydride site exchange. The dynamic processes at elevated temperatures are complicated by partial decomposition into $OsH(NO)(PPh_3)_3$. The hydride signal (but not the ^{31}P signal) of this species is unobservable at 120 °C, suggesting its involvement in the overall exchange process and preventing a reliable line-shape analysis.

Because neither **2a** nor **2c** exchanges hydrides with D_2 under ambient conditions, the hydride site exchange is intramolecular with respect to the hydrides. Furthermore, if the exchange is mediated by phosphine loss and is much faster for **2c** because of the weaker coordination ability of PPh_3 compared to P^iPr_3, **2c** should be readily converted to **2a** in the presence of excess P^iPr_3 at 20 °C. Because **2c** is inert to P^iPr_3 under these conditions, we conclude that the hydride site exchange in all of the trihydrides **2a**−**c** is nondissociative. Assuming that pairwise hydride site exchange, analogous to that in **1** (Scheme 2), operates in **2**, line-shape analysis of the ^1H NMR spectra of **2c** at 20 °C in CD_2Cl_2, in the absence of decomposition products, and of **2a** at 80 °C in d_8-PhMe gives k_{HH}(*mer*-**2c**,20°C) = 5 s^{-1} and k_{HH}(**2a**,80°C) = 3 s^{-1}, leading to $\Delta G^{\ddagger}_{HH}$(*mer*-**2c**,20°C) = 16 kcal/mol and $\Delta G^{\ddagger}_{HH}$(**2a**,80°C) = 20 kcal/mol. Therefore, with $\Delta S^{\ddagger}_{HH}$(**2**) ≈ 0, the values $\Delta H^{\ddagger}_{HH}$(*mer*-**2c**) = 16 kcal/mol and $\Delta H^{\ddagger}_{HH}$(**2a**) = 20 kcal/mol can be estimated.[63] The much faster exchange with the smaller and less electron-donating ligand PPh_3 is consistent with a transition state involving a small P−Os−P angle (≪180°), a dihydrogen $[OsH(NO)L_2](H_2)$ structure, or both.

DFT Calculations and Mechanisms of Hydride Site Exchange. (a) M = Ru. The lowest-energy mechanism of intramolecular hydride site exchange in the model *mer*-$Ru(H)_3(NO)(PH_3)_2$ found at the B3LYP/BS I level (Figure 5) consists of reductive coupling of two cis hydrides and H_2 ligand rotation in the resulting dihydrogen complex **C**-[RuNO] as the rate-determining step. This mechanism satisfies the following experimental results:

(a) The presence of a dihydrogen ligand in the rate-determining **TS(C)**-[RuNO] explains the inequality $\Delta H^{\ddagger}_{HH}$(**1a**) > $\Delta H^{\ddagger}_{HH}$(**1b**) as being caused by the (independently established) greater reducing ability of $RuH(NO)L_2$ toward H_2 with L = P^iPr_3 than with L = P^tBu_2Me. That is, the classical **B**-[RuNO] isomer is more stable than the nonclassical **TS(C)**-[RuNO] for the more reducing Ru with L = P^iPr_3.[57]

(b) The absence of significant heavy-ligand motion throughout the hydride site exchange (the phosphines remain mutually trans)

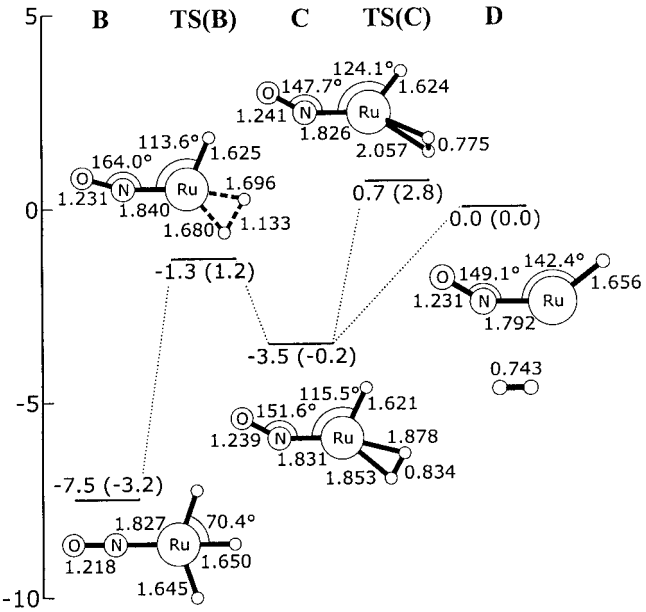

Figure 5. Selected geometrical parameters (Å, deg) and relative electronic energies (kcal/mol; those in parentheses are corrected with ZPE) of the structures involved in inter- and intramolecular hydride site exchange of *mer*,*trans*-$Ru(H)_3(NO)(PH_3)_2$, optimized at the B3LYP/BS I level and having essentially C_s or higher symmetry. Trans PH_3 groups were omitted for clarity. Labels in bold indicate the structural types, followed by -[RuNO] in the text, for example, **B**-[RuNO].

is consistent with the observation of exchange coupling in **1b**, a phenomenon that generally involves little to no rearrangement of the heavy ligand during the chemical exchange.[12]

(c) The computed $\Delta E^{\ddagger}_{HH}$ = 8.2 kcal/mol at this level compares well with the experimental value of $\Delta H^{\ddagger}_{HH}$ = 9.8(2) kcal/mol measured for **1b**.

However, the chosen level of theory fails to adequately describe the relative energetics of intra- and intermolecular hydride exchange. Experimentally, $\Delta H^{\ddagger}_1$(**1b**) ≥ 12 kcal/mol was estimated, whereas computationally, there is essentially no electronic energy barrier for H_2 coordination to **D**-[RuNO], and $\Delta E^{\ddagger}_1$ = ΔE_1 = 7.5 kcal/mol. Not only is the value of $\Delta E^{\ddagger}_1$ considerably lower than that of $\Delta H^{\ddagger}_1$(**1b**), but also $\Delta E^{\ddagger}_1$ < $\Delta E^{\ddagger}_{HH}$, such that intermolecular exchange with H_2 in **1** is predicted to be easier than intramolecular hydride site exchange, in sharp contrast to the experimental observations. This inconsistency can be attributed to a tendency of the B3LYP method to underestimate the binding of the H_2 ligand by an unsaturated metal center, as recently demonstrated in an Ir d^6 system.[50] Accordingly, increasing the donating ability of Ru in **D**-[RuNO] by using PMe_3 instead of PH_3 as the model phosphines lowers $\Delta E^{\ddagger}_{HH}$ from 0.7 kcal/mol above to 0.5 kcal/mol below $\Delta E^{\ddagger}_1$. In view of this methodological drawback, it should be noted that (a) the extent of H_2 ligand formation in **TS(C)**-[RuNO] may be overestimated and (b) the very shallow minimum **C**-[RuNO] may be a computational artifact, as we were unable to locate analogous nonclassical isomers **C** of **B**-$[RuCO]^-$ or **B**-[OsNO] (see below), with the much more reducing monohydrides **D** having very early and energetically low transition states for H_2 oxidative addition (Figure 6).

An alternative for the above site exchange mechanism involves the trigonal-bipyramidal **E**-[RuNO] isomer, which is nearly isoenergetic with **B**-[RuNO] (Figure 6), and cannot be strictly excluded as an intermediate for the hydride site exchange in **1**. However, compared to **TS(C)**-[RuNO], formation of **E**-[RuNO] from **B**-[RuNO] would similarly involve reductive

(62) Yandulov, D. V.; Caulton, K. G. Manuscript in preparation.

(63) Line-shape analysis under similarly slow exchange conditions in the case of **1b** gives k_{HH}(**1b**,−95°C) = 3.4 s^{-1}, which yields $\Delta G^{\ddagger}_{HH}$(**1b**,−95°C) = 9.8 kcal/mol, in excellent agreement with the value of $\Delta H^{\ddagger}_{HH}$(**1b**) obtained from the Eyring plot.

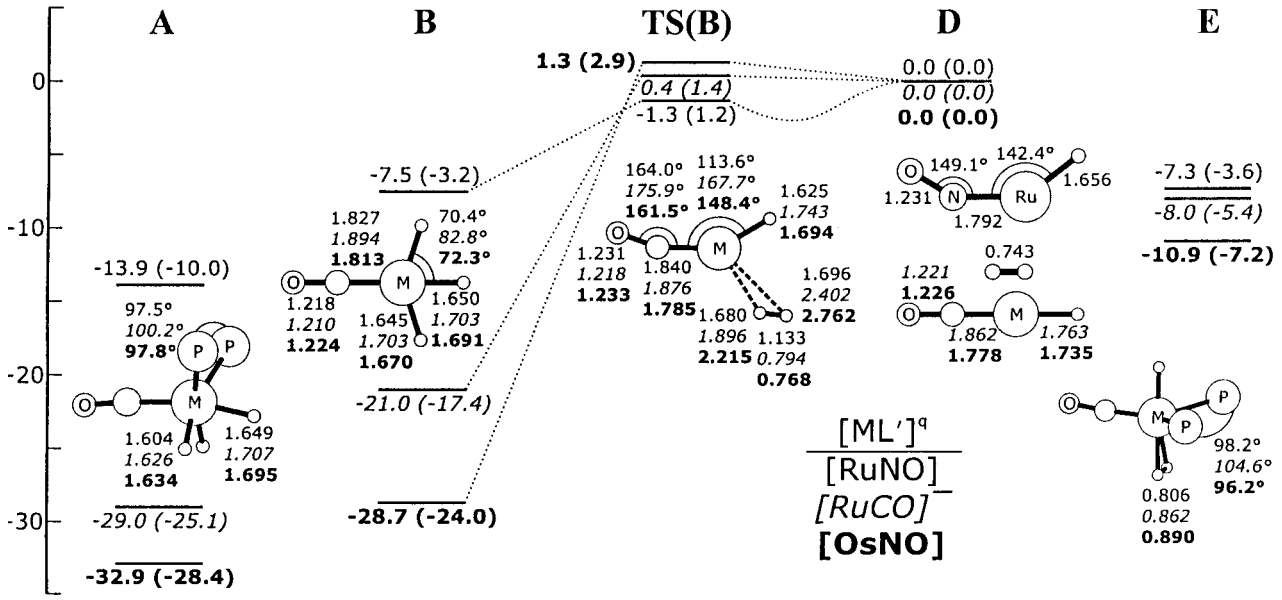

Figure 6. Selected geometrical parameters (Å, deg) and relative electronic energies (kcal/mol; those in parentheses are corrected with ZPE) of several $[ML']^qH_3(PH_3)_2$ isomers and structures involved in H_2 oxidative addition to *trans*-$[ML']^qH(PH_3)_2$, optimized at the B3LYP/BS I level and having essentially C_s or higher symmetry. PH_3 hydrogens and trans PH_3 groups were omitted for clarity. Labels in bold indicate the common structural types, followed by -$[ML']^q$ in the text when referring to specific structures, for example, **B**-$[RuCO]^-$. Cartesian coordinates of all optimized structures are provided in the Supporting Information.

coupling of cis hydrides and H_2 ligand rotation but would also require significant heavy-ligand motion, bending of the ∠P−Ru−P, and would thus be anticipated to have a higher activation energy than formation of **TS(C)**-[RuNO]. Additionally, the heavy-ligand motion required for the formation of the **E**-[RuNO] intermediate is an unlikely mechanistic feature in light of the observation of exchange coupling in **1b** (vide supra). Thus, considering both experimental and theoretical data, we conclude that intramolecular hydride site exchange in **1a** and **1b** proceeds via the dihydrogen **TS(C)**-[RuNO] transition state and possibly involves the nonclassical intermediate **C**-[RuNO].

(b) M = Os. Intramolecular hydride site exchange in d^6 pseudo-octahedral complexes is relatively uncommon and is known to occur via a limited number of mechanisms. These include (a) the "tetrahedral jump" of a single hydride in pseudo-octahedral structures distorted toward bicapped tetrahedra,[64] which has been extensively investigated[13,65] for *cis*-$M(H)_2L_4$ (M = Fe, Ru; L = PR_3) compounds; (b) the trigonal twist[66,67] of an octahedral face, which was established[19] for *cis*,*mer*-$Ru(H)_2(CO)(PPh_3)_3$; and (c) the reversible reductive coupling of two hydrides to form a trigonal-bipyramidal dihydrogen intermediate or a transition state, as detailed for *cis*,*trans*-$Re(H)_2(CO)(NO)L_2$[20] and *cis*-$M(H)_2(PP_3)$[21,22] (M = Co, Rh, Ir), which is formally analogous to the mechanism operating in **1**, but with unclear metal oxidation state assignments, that is, Ru(0) or Ru(II) in **C**-[RuNO] and **TS(C)**-[RuNO].

In the case of **2**, the two former exchange mechanisms, preserving the metal oxidation state, would proceed via *fac*- or *mer*,*cis*-$Os(H)_3(NO)L_2$ intermediates. At the B3LYP/BS I level, **A**-$[ML']^q$ is the global minimum geometry for $[ML']^q$ = [RuNO], $[RuCO]^-$, and [OsNO] (Figure 6), whereas *mer*,*cis*-$Os(H)_3(NO)(PH_3)_2$ is located only 4.6 kcal/mol (ΔE) above the mer, trans structure **B**-[OsNO]. Although steric bulk of the phosphines in the actual systems **2** makes the *mer*,*trans*-$Os(H)_3(NO)L_2$ isomer the global minimum, the local fac and mer, cis minima may remain energetically accessible from the mer, trans structure, within the range of the experimental value of $\Delta H^{\ddagger}_{HH}$ = 16−20 kcal/mol measured for **2a** and **2c**. For L = PPh_3, the fac isomer is found experimentally at only 2 kcal/mol ($\Delta G^{\circ}_{20^{\circ}C}$) above the mer structure, whereas for the bulkier L = P^iPr_3, *fac*-$[Os(H)_3(CO)L_2]^-$ can be stabilized over the mer isomer by ion pairing in solution.[32] The cis coordination of two L in the above hydride site exchange intermediates would then provide for the observed dependence of $\Delta H^{\ddagger}_{HH}$ on the steric bulk of L. Although we have not performed a thorough potential energy surface scan for isomerization of **B**-[OsNO], we note that in the case of the slowly exchanging[31] mixture of *mer*- and *fac*-$Ir(H)_3(CO)(PPh_3)_2$, the former isomer was shown[44] to undergo more rapid intramolecular hydride site exchange than that with free H_2 or with the fac isomer.

Alternatively, the hydride site exchange in **2** may involve the **E**-[OsNO] isomer (Figure 6), with a mechanism similar to that inferred for the closely related *cis*,*trans*-$Re(H)_2(CO)(NO)L_2$.[20] At the B3LYP/BS I level, **E**-[OsNO] is 16.8 kcal/mol [$\Delta(E + ZPE)$] above the mer isomer, comparable to the experimental range of $\Delta H^{\ddagger}_{HH}$ = 16−20 kcal/mol, and both steric and electronic factors would favor the dihydrogen structure more for L = PPh_3 than for L = P^iPr_3.

Discussion

Origin of Structural Distortions in *mer*-$M(H)_3(NO)L_2$. A Walsh diagram (Figure 7) for relaxation of the representative *mer*-$Os(H)_3(NO)(PH_3)_2$ optimized with angles within the *yz* plane constrained to 90° shows that three frontier orbitals of b_2 symmetry, Os d_{yz}, the H_A bonding combination, and NO π_z*, are primarily affected by the hydride bending. The distortion allows greater participation of the d_{yz} orbital in σ bonding with

(64) Hoffman, R.; Howell, J. M.; Rossi, A. R. *J. Am. Chem. Soc.* **1976**, *98*, 2484.
(65) Tebbe, F. N.; Meakin, P.; Jesson, J. P.; Muetterties, E. L. *J. Am. Chem. Soc.* **1970**, *92*, 1068. Meakin, P.; Muetterties, E. L.; Tebbe, F. N.; Jesson, J. P. *J. Am. Chem. Soc.* **1971**, *93*, 4701. Gerlach, D. H.; Peet, W. G.; Muetterties, E. L. *J. Am. Chem. Soc.* **1972**, *94*, 4545. Meakin, P.; Muetterties, E. L.; Jesson, J. P. *J. Am. Chem. Soc.* **1973**, *95*, 75. Jesson, J. P.; Meakin, P. *Acc. Chem. Res.* **1973**, *6*, 269.
(66) Bailar, J. C., Jr. *J. Inorg. Nucl. Chem.* **1958**, *8*, 165.
(67) Muetterties, E. L. *J. Am. Chem. Soc.* **1968**, *90*, 5097.

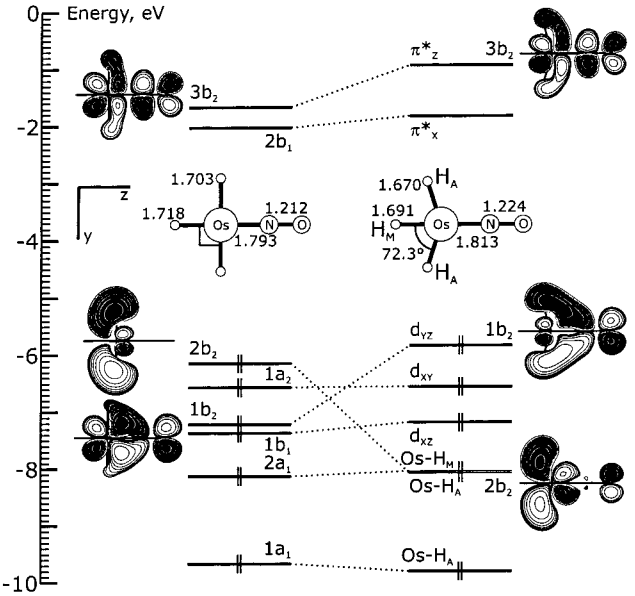

Figure 7. Walsh diagram showing the orbital origin of the hydride bending in *mer*,*trans*-$Os(H)_3(NO)(PH_3)_2$, which relates the fully optimized (B3LYP/BS I) structure (right) to the structure optimized with angles within the *yz* plane constrained to 90° (left), and selected geometrical parameters. The MO labels (C_{2v} symmetry) and nominal orbital characters are shown, along with graphical representation of the b_2-symmetry orbitals.

the H_A hydrides, which stabilizes $2b_2$, the bonding combination of H_A and Os $p_y + d_{yz}$, and destabilizes $1b_2$, the corresponding antibonding combination. Additional mixing-in of the vacant $3b_2$ (NO π_z*) orbital to both $1b_2$ and $2b_2$ is critical to the stability of the distorted structure and enhances back-bonding to NO. Without the π-accepting ability of NO, hydride bending would lead to a four-electron repulsion between the filled H_A b_2 combination and the Os d_{yz} orbital and would be much less pronounced. Thus, the resulting mixing of the b_2 orbitals in the distorted structure is essentially a "push−pull" interaction,[68] with the H_A b_2 σ-bonding combination acting as a filled π orbital and with α_{HH} being a structural manifestation of the extent of this interaction.

Pronounced changes in bond distances accompany the compression of α_{HH} (Figure 7). Substantial shortening of the Os−H_A bonds correlate with the stabilization of $2b_2$ on distortion and permits one to ascribe the major driving force for the hydride bending to stabilization of the Os−H_A σ bonds. By avoiding a mutually strong trans influence in the bent geometry, the H_A hydrides are able to better donate to the metal, as judged from the 0.05*e* increase in their Mulliken charges, forming shorter and stronger Os−H_A bonds. Because the Os d_{yz} orbital that becomes involved in Os−H_A σ bonding is filled, energetic stabilization on distortion is only possible with a concomitant increase in back-bonding to NO π_z*, which leads to a longer N−O bond and which raises the $3b_2$ in energy. In essence, bending of the H_A hydrides, driven by increased H_A-to-Os σ donation, "squeezes" the filled metal d_{yz} orbital into the vacant NO π_z*. A shortening of the Os−H_M bond by nearly as much as that of Os−H_A is unexpected and appears to occur mainly in response to the lengthening of the Os−N bond and, additionally, to the mixing of $2a_1$ and $1a_1$ in the distorted structure. The mixing of $1b_2$ and $2b_2$ rehybridizes Os d_{yz} toward NO in the Os−H_A antibonding $1b_2$, primarily involved in back-bonding to NO π* in the *yz* plane, which lengthens the Os−N bond to allow for better overlap of π_z* with the resulting d_{yz} orbital.

Analogous three-orbital four-electron interactions are involved in the bending of the equatorial carbonyls away from the apical CO in $[MH(CO)_5]^q$ (M = Cr^-, Mn)[14] and in the distortions of the phosphines away from the carbene in $OsX(=CHR)Cl(CO)L_2$[18] and from the CO in d^8 square-planar *trans*-$RhX(CO)L_2$.[69]

Distortions in *mer*-$[ML']^q(H)_3L_2$. Because hydride bending involves the strong mixing of *three* orbitals (Figure 7), the degree of distortion in a general *mer*-$[ML']^q(H)_3L_2$ complex will be difficult to predict, because varying M^q, L′, or L will generally affect the energies of all three participating orbitals. Nevertheless, an examination of trends within series of isoelectronic optimized structures (Table 4) reveals some features of ligand environment prerequisite for greater distortion. For constant $M^q = Os^-$, decreasing the π acidity of L′ along the series L′ = NO^+, CO, and PH_3 nearly eliminates the distortion, with α_{HH} increasing from 72.3° to 84.1°, whereas for both $M^q = Ru^-$ and M^q = Ir, a similar increase in α_{HH} is found on going from L′ = NO^+ to L′ = CO. At the same time, a slight decrease in α_{HH} is effected by varying M^q along the series $M^q = Re^{2-}$, Os^-, and Ir with constant L′ = NO^+. In each case, varying L′ or varying M^q, the less reducing ML′ is characterized by the smaller value of α_{HH}. Accordingly, the calculated value of α_{HH} is smaller for $M^q = Ru^-$ than for Os^- (L′ = NO^+) and for [OsNO] with the less-donating L = PH_3 than with PMe_3, consistent with experimental trends (**1a**,**b** vs **2a**,**b** and **2c** vs **2a**,**b**; Table 1): Ru is generally less reducing than Os, and the metal center is less electron-rich with weaker-donating phosphines. For a less-reducing M, there will be less back-bonding to the L′ π* orbital in the absence of the distortion, in a way, leaving more room for extra back-bonding that results from increased hydride bending. It is notable that varying L′ and its π acidity has the most pronounced consequences on α_{HH}, with the distortion reaching its maximum extent with the strongest π acid considered, NO^+, whereas changes in the intrinsic M−H bond lengths or the metal oxidation state, however dramatic, exert only a fine-tuning influence on α_{HH}. The opposite trends in α_{HH} calculated for the pairs $[OsCO]^-$ and $[RuCO]^-$ and $[OsCO]^-$ and [IrCO], that is, the more reducing M has the *smaller* value of α_{HH}, signify the complexity of factors that control modest distortions.

Distorting Ligands Other Than Hydrides. Because *mer*-$[ML']^q(H)_3L_2$ complexes are distorted in large part because of the H_A hydrides avoiding a mutually strong trans influence, the extent of distortion involving ligands other than H is expected to depend on their trans influences compared to that of H. In all of the optimized mer trihydrides (Table 4), trans PH_3 ligands are bent away from NO in the *xz* plane (Figure 7) with H_3P−M−H_M angles (α_{PH}) within the range of 81.2−84.6°. The distortion of the phosphines in the *xz* plane is analogous to that of the H_A hydrides in the *yz* plane and involves mixing of three corresponding b_1 orbitals. Although α_{PH} correlates with the π-accepting ability of L′ in a manner analogous to that of α_{HH}, both the absolute magnitude of the phosphine distortion and the relative changes in α_{PH} with L′ are considerably less pronounced than those resulting from hydride bending, consistent with PH_3 having a weaker trans influence than H. Although steric factors do not impede the distortion of the phosphines, as judged from [OsNO](PMe_3) having a value of α_{PH} 0.3° *smaller* than that of [OsNO](PH_3), "phosphine bending" must compete electronically with hydride bending for the limited

(68) Caulton, K. G. *New J. Chem.* **1994**, *18*, 25.
(69) Wierzbicki, A.; Salter, E. A.; Hoffman, N. W.; Stevens, E. D.; Van Do, L.; VanLoock, M. S.; Madura, J. D. *J. Phys. Chem.* **1996**, *100*, 11250.

Table 4. Selected Theoretical Values[a] for *mer*-$[ML']^q(H)_3(L)_2$

$[ML']^q$	α_{HH}	$M-H_M$[b]	$M-H_A$[c]	$\Delta E(-H_2)$	$\Delta E(O_h)$
[RuNO]	70.4 (72.5)[d]	1.650 (1.641)	1.645 (1.647)	7.5 (6.1)	10.7
$[RuCO]^-$	82.8	1.703	1.703	21.0	*e*
[OsNO]	72.3 (73.9)	1.691 (1.682)	1.670 (1.668)	28.7	10.4
$[OsNO](PMe_3)_2$	73.0	1.697	1.673	*e*	*e*
$[OsCO]^-$	81.3 (82.1)	1.732 (1.724)	1.710 (1.706)	40.6	2.6
$[OsPH_3]^-$	84.1	1.671	1.718	49.3	0.7
$[ReNO]^-$	74.6	1.774	1.720	*e*	*e*
$[IrNO]^+$	71.5	1.625	1.642	*e*	*e*
[IrCO]	84.0	1.649	1.675	12.8	*e*

[a] Angles (deg), distances (Å), and electronic energies for H_2 loss, $\Delta E(-H_2)$, and stabilization relative to the geometry optimized with α_{HH} constrained to 90°, $\Delta E(O_h)$, in kcal/mol at B3LYP/BS I with L = PH_3, unless otherwise indicated. [b] Hydride trans to NO. [c] Hydrides cis to NO. [d] BS II values are given in parentheses. [e] Not calculated.

overall π-accepting ability of L′. Optimization of *mer*-$M(H)_3(NO)(PH_3)_2$ with angles in the *yz* plane constrained to 90° leads to values of α_{PH} = 76.5° (Ru) and 78.6° (Os), 4.8° and 3.1° smaller, respectively, than in the fully optimized structures. Thus, (a) the distortion is inherently less pronounced with the weaker trans influencing PH_3, than with H; (b) the distortion of the H_A hydrides dominates the back-bonding to NO, because the N−O bond lengthens with decreasing α_{HH} (Figure 7) despite increasing α_{PH}; and (c) the stabilization energy relative to the structure optimized with α_{HH} constrained to 90° (Table 4) is somewhat underestimated, because structures with α_{HH} = 90° are stabilized by greater phosphine bending.

Diminishing the trans influence of the ligands involved in the distortion even further effectively turns off the distortion, even with L′ being as strong a π acceptor as NO^+. Thus, X-ray structure determinations of *mer*-$RuCl_3(NO)L_2$ (L = PPh_2Me,[70] PPh_3[71]) and *mer*-$[OsCl_3(NO)(SnCl_3)_2][PPh_4]_2$[72] reveal essentially no distortions from octahedral geometry with cis Cl−M−Cl angles within the 88.15(6)−92.16(6)° range for Ru and 86.8(1)° for Os, reproduced well at the B3LYP/BS I level with *mer*-$MCl_3(NO)(PH_3)_2$ as 88.5° (Ru) and 87.3° (Os). In addition to the weak trans influence of the chloride ligands, the distortion is absent in *mer*-$MCl_3(NO)L_2$ because of steric repulsion between the Cl ligands[73] and push−pull interactions[68] involving all three π-donating Cl and NO ligands, which benefit from the linearity of Cl_A-M-Cl_A and Cl_M-M-NO.

Summary of the Factors Dictating the Distortion. Overall, geometrical distortions in a pseudo-octahedral d^6 ML_6 complex of the type exemplified by *mer*-$M(H)_3(NO)L_2$ (M = Ru, Os) require (a) two trans ligands with strong trans influence (b) that are located cis to a strong π acceptor (c) in the absence of impeding steric or electronic factors. Complexes **1** and **2** investigated here fit the profile rather well, and even greater distortion can probably be achieved with a π acid stronger than NO^+, perhaps a single-face π-acceptor singlet alkylidene.

Comparison to $d^{n<6}$ ML_6. Structural distortions from octahedral geometry in ML_6 complexes involving strong σ donors and driven primarily by electronic factors are well documented. Studied both experimentally and theoretically, d^0 $[MMe_6]^q$ (M = W, Nb^-, Ta^-)[1,2] complexes adopt structures derived from a trigonal prism, as predicted for a number of other metal hexamethyls and hexahydrides,[3,74−76] whereas ∠H−M−H in d^0 *trans*,*trans*-$Ta(H)_2(L)X(OR)_2$[5,6,77] is substantially less than 180°. The d^1 $ReMe_6$[1,2] is nonoctahedral, similar to the d^0 analogues, as are the calculated d^1 MMe_6 (M = Tc, Re) and d^2 MMe_6 (M = Ru, Os)[3], whereas in d^2 $Cp^*Os(H)_5$ four equatorial hydrides are strongly bent away from the Cp* ligand.[78,7] Finally, the d^4 $Os(H)_2Cl_2L_2$[4] has a trigonal-prismatic structure distorted from the electronically preferred bicapped-octahedral arrangement[79] by steric factors,[80] whereas d^4 *mer*-$Os(H)_3XL_2$[8,10] and *mer*-$OsHCl_3L_2$[9] have transoid H−Os−H and L−Os−L units, respectively, strongly deviating from linearity. Whereas for d^2 and d^4 ML_6 complexes octahedral structure is incompatible with a diamagnetic state, in all of the above examples the distortion is in large part driven by a strengthening of the M−L σ bonds via involvement of vacant metal d orbitals and additionally reinforced by increased π donation from halides in unsaturated cases. In this regard, the distortion in **1** and **2** is unusual, because it occurs with a d^6 metal configuration and it is a combination of a filled metal d orbital and a vacant NO π* orbital that acts as a vacant metal d orbital to participate in σ bonding with the bending hydrides. Hence, the extent of distortion and the energetic stabilization that results from it are both less pronounced than those involving truly vacant d orbitals, and they are highly sensitive to the π acidity of L′ (Table 4). The electronic structure of *mer*-$Os(H)_3(NO)L_2$ is qualitatively analogous to those of d^4 *mer*-$Os(H)_3XL_2$[10] and d^0 *trans*,*trans*-$Ta(H)_2(L)X(OR)_2$,[6] in which the transoid hydrides are similarly bent away from the π donor X, except that hydride bending reinforces the M ← X π donation rather than the M → NO π back-bonding. These can be considered hole/electron equivalents, or[81,82] alternatively, the difference is only one of whether the electrons "originate" from the metal (Os−NO) or the ligand (Os−Cl, Ta−Cl). However, the distortion in $d^{n<6}$ species is greater (α_{HH} = 60° for Os[10] and α_{HL} = 63−69° for Ta[77]) and provides >25 kcal/mol stabilization relative to the pseudo-octahedral structures, as calculated for Ta, and the α_{HL} values calculated for Ta differ by only 3° between X = strong π donor; NH_2^-; and pure σ donor, hydride.

Energetic Stabilization of *mer*-$[ML']^q(H)_3L_2$. The energies of the fully optimized mer trihydrides relative to those optimized

(70) Schultz, A. J.; Henry, R. L.; Reed, J.; Eisenberg, R. *Inorg. Chem.* **1974**, *13*, 732.
(71) Haymore, B. L.; Ibers, J. A. *Inorg. Chem.* **1975**, *14*, 3060.
(72) Czeska, B.; Weller, F.; Dehnicke, K. *Z. Anorg. Allg. Chem.* **1983**, *498*, 121.
(73) Ujaque, G.; Maseras, F.; Eisenstein, O. *Theor. Chim. Acta* **1997**, *96*, 146.
(74) Demolliens, A.; Jean, Y.; Eisenstein, O. *Organometallics* **1986**, *5*, 1457.
(75) Kang, S. K.; Albright, T. A.; Eisenstein, O. *Inorg. Chem.* **1989**, *28*, 1611.
(76) Kang, S. K.; Tang, H.; Albright, T. A. *J. Am. Chem. Soc.* **1993**, *115*, 1971.
(77) Bayse, C. A.; Hall, M. B. *Organometallics* **1998**, *17*, 4861.
(78) Bayse, C. A.; Couty, M.; Hall, M. B. *J. Am. Chem. Soc.* **1996**, *118*, 8916.
(79) Gusev, D. G.; Kuhlman, R.; Rambo, J. R.; Berke, H.; Eisenstein, O.; Caulton, K. G. *J. Am. Chem. Soc.* **1995**, *117*, 281.
(80) Maseras, F.; Eisenstein, O. *New J. Chem.* **1998**, *22*, 5.
(81) Cayton, R. H.; Chisholm, M. H.; Clark, D. L.; Hammond, C. E. *J. Am. Chem. Soc.* **1989**, *111*, 2751.
(82) Chisholm, M. H.; Clark, D. L.; Hampden-Smith, M. J.; Hoffman, D. H. *Angew. Chem.* **1989**, *101*, 446.

with $\alpha_{HH} = 90°$ [$\Delta E(O_h)$, Table 4] provide an estimate of the energetic importance of hydride bending. The $\Delta E(O_h)$ values reach a maximum of 10 kcal/mol with the strongest π acid, NO^+, for [RuNO] and [OsNO], indicating a relatively pronounced energetic preference for the distorted structure, and drop sharply with increasing α_{HH} (Table 4). *For a given metal*, there is a clear correlation between α_{HH} and $\Delta E(-H_2)$ for H_2 loss (Table 4), not surprisingly, as both are strongly dependent on the π acidity of L′.

The energetic stabilization of *mer*-$[ML']^q(H)_3L_2$ that results from hydride bending also affects the relative stability of the mer and fac isomers. Although the distortion in the mer geometry (**B**) alleviates the mutual trans influence of the H_A hydrides, in all of the systems considered (Figure 6) the fac isomer (**A**), in which two hydrides are transoid to ligands with a weaker trans influence (phosphines), is more stable, in the absence of actual steric effects. The fac geometry is additionally stabilized by the bending of transoid H−M−P units, analogous to that of H_A-M-H_A and P−M−P units in the mer geometry, with the optimized ∠H−M−P = 155.3°, 163.0°, and 157.0°, respectively, in the **A**-[RuNO], -$[RuCO]^-$, and -[OsNO] series (Figure 6). However, because the H−M−P bending involves ligands with weaker trans influence than does H_A-M-H_A distortion, the latter is expected to be more pronounced (vide supra) for a given $[ML']^q$ and thus to stabilize the mer isomer more than the fac isomer for a stronger π acid L′, assuming that the relative energies of strictly octahedral *mer*- and *fac*-$[ML']^q(H)_3L_2$ complexes are only weakly dependent on the nature of $[ML']^q$. Indeed, the mer isomer is stabilized relative to the fac by 1.6 kcal/mol (ΔE) on going from $[RuCO]^-$ to [RuNO] (Figure 6), the experimental fac ↔ mer equilibrium constant is at least an order of magnitude greater for $Os(H)_3(NO)(PPh_3)_2$ (**2c**) than for $Ir(H)_3(CO)(PPh_3)_2$[31] and for $[Re(H)_3(NO)(P^iPr_3)_2]^-$ than for $[M(H)_3(CO)(P^iPr_3)_2]^-$ (M = Ru, Os).[32] Additionally, $[Ru(H)_3(PPh_3)_3]^-$, for which essentially no stabilization is possible (compare $[OsPH_3]^-$, Table 4), exists exclusively as the fac isomer.[83,84] These experimental results are consistent with energetic stabilization of the transoid dihydride configuration (the mer isomer) via hydride bending.

Effects on the Intramolecular Hydride Site Exchange in 1. Perhaps the most important outcome of the structural distortion present in **1** and **2** is the observation of quantum mechanical exchange coupling in the case of *mer*-$Ru(H)_3(NO)(P^tBu_2Me)_2$ (**1b**), as well as its disappearance in the closely related (only slightly perturbed) analogue **1a**. Because the transition state for the chemical hydride site exchange in **1** is a dihydrogen complex **TS(C)**-[RuNO], the distortion of the ground-state geometry, which decreases the $H_A\cdots H_M$ distance, shortens the tunneling path (narrows the barrier) and, thus, increases the tunneling rate, leading to observable exchange coupling for **1b**. The transition state for the chemical site exchange in transition metal polyhydrides that exhibit exchange coupling generally[12] involves some shortening of the distance between the exchanging hydrides; a dihydrogen structure suffices, but is not necessary, since the potential energy surface for H−H stretching can be very flat.[10] Thus, the case of **1b** is no exception, as both experimental and computational results strongly support the nonclassical structure of the transition state for the exchange in **1**. However, because none of the numerous polyhydrides[12] exhibiting exchange coupling between hydride ligands has a strictly octahedral structure, or at least one with $\alpha_{HH} \approx 90°$, the case of **1b** signifies the importance of bringing the exchanging hydrides closer together in the ground-state structure to the observation of exchange coupling. It also demonstrates the existence of exchange coupling with H···H distances as long as 2 Å (Table 1), albeit considerably less pronounced for the given value of $\Delta H^{\ddagger}_{HH}$.[12]

The combination of the strong π acidity of NO^+ and the moderate reducing ability of Ru(II) keeps the dihydrogen **TS(C)**-[RuNO] structure close in energy to the trihydride **B**-[RuNO] structure (Figure 5) and is responsible for the facile chemical hydride site exchange observed in **1**. In this regard, the hydride bending in *mer*-$M(H)_3(NO)L_2$ (M = Ru, Os) makes the trihydride structure "prepared" to reductively couple cis hydrides: the distortion not only brings the H_A and H_M hydrides closer and diminishes the nucleophilicity of H_A but also increases back-bonding to NO, both of which are developed further in **TS(B)**-[MNO] and **TS(C)**-[RuNO] as the formation of the H_2 ligand and as partial NO bending (Figures 5 and 6). In a way, the distorted structures of mer trihydrides of Ru and Os can be viewed as "arrested" on the H_2 oxidative addition pathway. Thus, given the moderate reducing ability of Ru, the hydride bending in **B**-[RuNO] helps lower the barrier for the hydride site exchange to within the range commonly measured[12] for complexes that exhibit exchange coupling. Given the very high sensitivity of the exchange coupling magnitude to the barrier height and width[12] and the relatively small J_{HH} values observed in **1b**, it is not surprising to find that even a slight increase in the donating ability of L on going from L = P^tBu_2Me (**1b**) to L = P^iPr_3 (**1a**) effectively shuts down the exchange coupling, because of both raising and widening the barrier for the chemical exchange (vide supra).

Generalization to Dihydrides. The phenomenon of hydride bending is not limited to d^6 mer trihydrides, in which trans H−M−H units are distorted from linearity. An analogous (eq 2) T_{1min} approach in the case of *cis*,*trans*-$Os(H)_2Cl(NO)(P^iPr_3)_2$ yields[85] $\alpha_{HH} = 76(3)°$ (Table 1), reproduced as 72.7° at the B3LYP/BS I level with *cis*,*trans*-$Os(H)_2Cl(NO)(PH_3)_2$. The optimized structure shows that the compression of α_{HH} from 90° is largely compensated by the expansion of ∠Cl−Os−N, such that the cis H−Os−N and H−Os−Cl angles remain approximately 90°. The distortion is reminiscent of the one investigated computationally[74] for d^0 $[Ti(H)_6]^{2-}$ and results in a feature common to the distortion in **1** and **2**: the transoid H−Os−L angles, ∠H−Os−Cl = 158.3° and ∠H−Os−N = 161.7°, are well below 180°. The essential rationale behind this distortion is similar to that discussed for mer trihydrides and consists of strengthening the Os−H σ bonds by moving the hydrides away from the trans ligands and increasing the π back-bonding to NO, which, because of the asymmetry of the structure, leads to a bending of ∠Os−N−O in the direction of the cis hydride to a value of 164.7°.

A thorough T_1 relaxation study[86] of the isoelectronic *cis*,*trans*-$Re(H)_2(CO)(NO)(PR_3)_2$ revealed an analogous distortion, $\alpha_{HH} = 80°$, later reproduced computationally[87] (DFT) as $\alpha_{HH} = 77-79°$, that was compensated by expansion of ∠C−Re−N similar to that in *cis*,*trans*-$Os(H)_2Cl(NO)(P^iPr_3)_2$. Therefore, at least in the presence of the very strong π acceptor NO^+, significant distortions are possible in cis dihydrides with d^6 metal configuration as well, driven by increased H-to-M σ donation

(83) Chan, A. S. C.; Shieh, H.-S. *J. Chem. Soc., Chem. Commun.* **1985**, 1379.
(84) Pez, G. P.; Grey, R. A.; Corsi, J. *J. Am. Chem. Soc.* **1981**, *103*, 7528.
(85) Os−H distances of 1.626 and 1.674 Å were taken from a B3LYP/BS I calculation on the model *cis*,*trans*-$Os(H)_2Cl(NO)(PH_3)_2$.
(86) Gusev, D. G.; Nietlispach, D.; Vymenits, A. B.; Bakhmutov, V. I.; Berke, H. *Inorg. Chem.* **1993**, *32*, 3270.
(87) Jacobsen, H.; Jonas, V.; Werner, D.; Messmer, A.; Panitz, J.-C.; Berke, H.; Thiel, W. *Helv. Chim. Acta* **1999**, *82*, 297.

and π back-bonding to NO^+. However, this d^6 species, which shows no hydride site exchange, shows no exchange coupling. Notably, facile hydride site exchange was reported[88] to occur in the closely related species *cis,trans*-$[Os(H)_2(CO)(NO)(PR_3)_2]^+$, with $\Delta G^{\ddagger}_{HH} = 12.7$ (R = Cy) and 11.6 (R = Ph) kcal/mol. In anticipation of a trigonal-bipyramidal dihydrogen intermediate that mediates the exchange, by analogy to the isoelectronic neutral rhenium system,[20] and a structure similarly distorted by compression of α_{HH}, ^1H NMR spectra of the cationic osmium complexes may exhibit small exchange couplings.

Conclusions

mer-$M(H)_3(NO)L_2$ (M = Ru, Os) complexes adopt pseudo-octahedral structures significantly distorted by compression of the cis H−M−H angles to ∼75°, as inferred from ^1H NMR T_{1min} and IR data and from DFT calculations. Calculations additionally suggest that this structural feature is common to other nitrosyl polyhydrides. Strong back-bonding interactions with linear NO are responsible for the distortion, allowing the H_A hydrides to avoid a mutually strong trans influence. The stabilizing influence of the distortion is evident in the slight stabilization of the mer relative to the fac isomers.

Although strong back-donation to the NO π^* orbital increases the chance of achieving reversible NO bending via full transfer of two electrons (an intramolecular redox process), the osmium complexes **2** do not exhibit associative reactivity under moderate conditions. The ruthenium analogues **1** undergo facile intramolecular hydride site exchange, for which both experimental and theoretical results strongly suggest a dihydrogen transition state. In this regard, the distortion makes the trihydride structure "prepared" to reductively couple two cis hydrides and facilitates the hydride site exchange in **1**. Additionally, the distortion shortens the hydride tunneling path, which makes moderate exchange coupling observable in **1b**, the first d^6 pseudo-octahedral polyhydride to exhibit such a phenomenon. Whereas ruthenium trihydrides easily lose H_2, osmium complexes, being inherently more reducing, are much more stable toward H_2 reductive elimination and also undergo intramolecular hydride site exchange, albeit with a considerably higher activation energy.

Finally, the distortion identified for mer trihydrides **1** and **2** is not limited to d^6 structures with transoid hydrides, but also exists in cis dihydrides $Os(H)_2Cl(NO)L_2$ and $Re(H)_2(CO)(NO)L_2$ in which the cis H−M−H angles are similarly compressed to ≤80°.

Experimental Section

General. All manipulations were carried out using standard Schlenk and glovebox techniques under argon. Bulk solvents were purified by appropriate methods, as follows: 2-methoxyethanol was deoxygenated; pentane, heptane, benzene, THF, and Et_2O were dried over sodium benzophenone ketyl; and methanol and ethanol were dried over magnesium methoxide and calcium ethoxide, respectively. All were then distilled under Ar, and stored over 3- or 4-Å molecular sieves in gastight solvent bulbs with Teflon closures. d_6-Benzene, d_8-toluene, and d_{10}-Et_2O were dried over Na metal, CD_2Cl_2 was dried over calcium hydride, and $CDCl_3$ was dried over calcium chloride; all were then vacuum transferred, degassed, and stored in Teflon-stoppered bulbs in an argon-filled glovebox. *N*-Methyl-*N*-nitroso-*p*-toluenesulfonamide, isoamyl nitrite (97%), silver trifluoromethanesulfonate, sodium borohydride, triethylamine trihydrofluoride (98%), trifluoromethanesulfonic acid (Aldrich Chemical Co.), H_2 (UHP/zero grade, Air Products), D_2 (99.8% D, Cambridge Isotope Laboratories), P^iPr_3 (>90%, Strem Chemicals), and $OsCl_3 \cdot nH_2O$ (52−56% Os, Pressure Chemicals) were used as received. The complexes *trans*-$RuMe(NO)L_2$ (L = P^iPr_3, P^tBu_2Me) were prepared as reported.[40] ^1H, ^{31}P, and ^{19}F NMR spectra were recorded on a Varian Gemini 2000 (^1H, 300 MHz; ^{31}P, 122 MHz; ^{19}F, 282 MHz) or a Varian Inova 400 (^1H, 400 MHz; ^{31}P, 162 MHz; ^{19}F, 376 MHz) spectrometer and referenced to the residual protio solvent peaks (^1H) or to an external 85% H_3PO_4 (^{31}P) and C_6D_6 solution of CF_3COOH (^{19}F, −78.9 ppm relative to $CFCl_3$). Chemical shifts are reported in parts per million relative to tetramethylsilane (^1H), 85% H_3PO_4 (^{31}P), and $CFCl_3$ (^{19}F). Temperatures from ambient to −100 °C were calibrated with a methanol standard and extrapolated to lower temperatures. During VT measurements, samples were allowed at least 10 min to equilibrate at each temperature, which was maintained to ±0.5 °C. Infrared spectra were recorded on a Nicolet 510P FT-IR spectrometer. Numerical data analyses were performed with Matlab 5.3.[89] All error analyses used standard error propagation formulas,[90] that is, for $f = f(x_1, x_2, ...)$, $\sigma(f)^2 = (\partial f/\partial x_1)^2\sigma(x_1)^2 + (\partial f/\partial x_2)^2\sigma(x_2)^2 + ...$, neglecting the covariance terms.

***cis,trans*-Os(H)$_2$Cl(NO)(P^{i}Pr$_3$)$_2$.** A 500-mL Fisher−Porter bottle was charged with $OsCl_3 \cdot nH_2O$ (1.000 g, 2.84 mmol), THF (50 mL), and P^iPr_3 (2.530 g, 14.2 mmol). The mixture was pressurized with H_2 (25 psi, ∼31.24 mmol) and vigorously stirred at 90 °C for 16 h, yielding a dark-red solution of $OsH_2Cl_2(P^iPr_3)_2$. After the mixture had cooled to RT, the excess pressure was released against Ar flow, and Et_3N (1.724 g, 17.04 mmol) and isoamyl nitrite (0.377 g, 3.12 mmol) were added rapidly and successively in an Ar-filled glovebox, producing a yellow, heterogeneous mixture. The mixture was pressurized with H_2 (25 psi), stirred at RT for an additional 30 min, transferred in a Schlenk flask, and brought to dryness. The solid residue was extracted with pentane (7 × 10 mL), and the combined extracts were filtered through Celite and concentrated to ∼15 mL to yield a golden-brown, analytically pure crystalline material after several days at −40 °C. This material was washed with cold pentane (3 × 10 mL) and dried in vacuo. Yield: 1.330 g (2.30 mmol, 81%). Spectroscopic data have been reported previously.[41]

***cis,trans*-Os(H)$_2$Cl(NO)(P^{t}Bu$_2$Me)$_2$.** A procedure analogous to that employed for the P^iPr_3 analogue, starting from $OsCl_3 \cdot nH_2O$ (0.500 g, 1.42 mmol), THF (25 mL), and P^tBu_2Me (95%, 1.200 g, 7.11 mmol) in an 85-mL Fisher−Porter bottle under H_2 (60 psi, ∼9.94 mmol) at 90 °C for 16 h and using Et_3N (0.862 g, 8.52 mmol) and isoamyl nitrite (0.189 g, 1.56 mmol), yielded 0.630 g (1.09 mmol, 77%) of a golden-brown, crystalline material. ^1H NMR (C_6D_6, 20 °C): δ 1.53 [vt, N = 7.0 Hz, 6H, $PCH_3(^tBu)_2$], 1.27 [vt, N = 13.2 Hz, 18H, $PMe(C(CH_3)_3)_2$], 1.26 [vt, N = 13.2 Hz, 18H, $PMe(C(CH_3)_3)_2$], −1.64 (td, J_{PH} = 21.9 Hz, J_{HH} = 7.3 Hz, 1H, Os*H*), −10.55 (td, J_{PH} = 14.6 Hz, J_{HH} = 7.3 Hz, 1H, Os*H*). $^{31}P\{^1H\}$ NMR (C_6D_6, 20 °C): δ 28.3 (s). IR (C_6H_6): 1697 cm^{-1} (ν_{NO}).

OsCl$_3$(NO)(PPh$_3$)$_2$. A modification of the reported procedure[91] was used. Solutions of $OsCl_3 \cdot nH_2O$ (0.350 g, 0.99 mmol) and *N*-methyl-*N*-nitroso-*p*-toluenesulfonamide (0.426 g, 1.99 mmol), both in 15 mL of 2-methoxyethanol, were simultaneously added via cannulas to a refluxing solution of PPh_3 (1.564 g, 5.96 mmol) in 40 mL of 2-methoxyethanol, leading to the formation of a fine brown precipitate within 5−10 min. The mixture was refluxed for a total of 20 min and cooled to RT. The brown solution was decanted off, and the brown solid was washed with 2-methoxyethanol (3 × 10 mL) and Et_2O (3 × 10 mL) and dried in vacuo. Yield: 0.600 g (0.70 mmol, 71%). The product is very poorly soluble in C_6D_6 or CD_2Cl_2. ^1H NMR (CD_2Cl_2, 20 °C): δ 7.83 [m, 12H, P(*o*-C_6H_5)$_3$], 7.45 [m, 18H, P(*p,m*-C_6H_5)$_3$]. $^{31}P\{^1H\}$ NMR (CD_2Cl_2, 20 °C): δ −15.3 (s). IR (Nujol mull): 1850 cm^{-1} (ν_{NO}).[91]

***mer,trans*-Os(H)$_3$(NO)(P^{i}Pr$_3$)$_2$ (2a).** *cis,trans*-$Os(H)_2Cl(NO)(P^iPr_3)_2$ (0.300 g, 0.52 mmol) and $NaBH_4$ (98.2 mg, 2.6 mmol) were placed in

(88) Johnson, B. F. G.; Segal, J. A. *J. Chem. Soc., Dalton Trans.* **1974**, 981.

(89) *MATLAB*, version 5.3.0.10183 (R11); The MathWorks, Inc.: Natick, MA, copyright 1984−1999.

(90) Bevington, P. R. *Data Reduction and Error Analysis for the Physical Sciences*; McGraw-Hill Book Company: New York, 1969; Chapter 4.

(91) Ahmad, N.; Levison, J. J.; Robinson, S. D.; Uttley, M. F. *Inorg. Synth.* **1974**, *15*, 45.

an 85-mL Fisher−Porter bottle. Methanol (12 mL) was rapidly added, and the bottle was promptly capped. The solution, becoming lighter in color, was stirred under the resulting H_2 pressure of 40 psi (∼8 mmol) at 90 °C for 14 h, transferred in a Schlenk flask, and brought to dryness. The solid residue was extracted with pentane (4 × 5 mL), and the combined extracts were filtered through Celite and brought to dryness again. The resulting yellow solid was recrystallized from methanol at −40 °C to give a bright yellow, crystalline material, which was washed with cold methanol and dried in vacuo. Yield: 0.210 g (0.39 mmol, 74%). X-ray-quality crystals were obtained from the reaction mixture after it was allowed to stand for several hours at RT. ^{1}H NMR (C_6D_6, 20 °C): δ 2.01 [m, 6H, P(C*H*$(CH_3)_2)_3$], 1.19 [dvt, J_{HH} = 6.9 Hz, N = 13.8 Hz, 36H, P(CH(C*H*$_3)_2)_3$], −7.26 (td, J_{PH} = 15.8 Hz, J_{HH} = 6.3 Hz, 2H, OsH_A), −9.67 (tt, J_{PH} = 25.2 Hz, J_{HH} = 6.3 Hz, 1H, OsH_M). ^{31}P{^{1}H} NMR (C_6D_6, 20 °C): δ 45.3 (s). IR (C_6D_6): 1673 cm^{-1} (ν_{NO}).

***mer,trans*-Os(H)$_3$(NO)(P^{t}Bu$_2$Me)$_2$ (2b).** A procedure identical to that used for **2a** gave 0.220 g (0.40 mmol, 78%) of the product as a bright yellow, crystalline solid. ^{1}H NMR (C_6D_6, 20 °C): δ 1.56 [vt, N = 6.0 Hz, 6H, PC*H*$_3$(^{t}Bu)$_2$], 1.29 [vt, N = 13.2 Hz, 18H, PMe(C(C*H*$_3)_3)_2$], −6.78 (td, J_{PH} = 15.4 Hz, J_{HH} = 6.2 Hz, 2H, OsH_A), −8.49 (tt, J_{PH} = 24.5 Hz, J_{HH} = 6.2 Hz, 1H, OsH_M). ^{31}P{^{1}H} NMR (C_6D_6, 20 °C): δ 37.5 (s). IR (C_6D_6): 1670 cm^{-1} (ν_{NO}).

Os(H)$_3$(NO)(PPh$_3$)$_2$ (2c). A 50-mL Schlenk flask fitted with a Teflon valve was charged with $OsCl_3(NO)(PPh_3)_2$ (0.170 g, 0.20 mmol), $NaBH_4$ (0.134 g, 3.0 mmol), and EtOH (15 mL). The mixture was vigorously stirred at 90 °C for 22 h and cooled to RT. The brown solution was decanted off, and the brown solid was washed with EtOH (2 × 10 mL) and Et_2O (3 × 10 mL, until the washes were colorless). The resulting yellow solid was extracted with C_6H_6 (3 × 5 mL), and the combined extracts were filtered through Celite, concentrated to ∼2 mL, and layered with Et_2O (20 mL) for several hours, producing yellow crystals, which were rinsed with Et_2O and dried in vacuo. Yield: 35 mg (0.05 mmol, 23%). The *mer*-**2c** and *fac*-**2c** isomers were observed in a constant ∼95:5 ratio throughout several days at 20 °C in C_6D_6 and after heating the solution to ∼100 °C, which leads to complete averaging of the hydride resonances, although slow establishment of the equilibrium cannot be ruled out because of the very weak intensity of the *fac*-**2c** hydride signals. *mer*-**2c**. ^{1}H NMR (C_6D_6, 20 °C): δ 7.86 [m, 12H, P(*o*-$C_6H_5)_3$], 6.99 [m, 18H, P(*p*,*m*-$C_6H_5)_3$], −4.94 (td, J_{PH} = 17.2 Hz, J_{HH} = 5.3 Hz, 2H, OsH_A), −6.11 (tt, J_{PH} = 26.1 Hz, J_{HH} = 5.3 Hz, 1H, OsH_M). ^{31}P{^{1}H} NMR (C_6D_6, 20 °C): δ 18.7 (s). IR (C_6D_6): 1703 cm^{-1} (ν_{NO}). *fac*-**2c**. ^{1}H NMR (C_6D_6, 20 °C, hydride region, AA′M part of the AA′MXX′ spin system): δ −4.10 [m, J(P−H)$_{cis}$ = ±18.8 Hz, J(P−H)$_{trans}$ = ∓71.6 Hz, J(H$_A$−H$_M$) = 4.7 Hz, 2H, AA′], −5.44 [tt, J_{PH} = 27.0 Hz, J(H$_A$−H$_M$) = 4.7 Hz, 1H, M]. ^{31}P{^{1}H} NMR (C_6D_6, 20 °C): δ 11.6 (s).

***cis,trans*-Os(H)$_2$(O$_3$SCF$_3$)(NO)(P^{i}Pr$_3$)$_2$.** A modification of an earlier procedure[42] was used. A Schlenk flask was charged with *cis*,*trans*-$Os(H)_2Cl(NO)(P^iPr_3)_2$ (1.000 g, 1.73 mmol) and AgOTf (0.441 g, 1.70 mmol). Ether (15 mL) was added, and the resulting mixture was stirred in the dark for 1 h, filtered through Celite, concentrated to ∼1 mL, and layered with pentane (30 mL) overnight to yield dark orange crystals, which were rinsed with pentane and dried in vacuo. Yield: 1.040 g (1.50 mmol, 89%). Spectroscopic data have been reported previously.[42]

***cis,trans*-Os(H)$_2$(O$_3$SCF$_3$)(NO)(P^{t}Bu$_2$Me)$_2$.** The product is sensitive to AgCl at RT. A Schlenk flask was charged with *cis*,*trans*-$Os(H)_2Cl(NO)(P^tBu_2Me)_2$ (0.200 g, 0.35 mmol) and AgOTf (88.0 mg, 0.34 mmol) and cooled to −13 °C. Ether (10 mL) was slowly added, and the resulting mixture was stirred in the dark at −13 °C for 40 min and filtered through Celite. The volatiles were removed in vacuo, the resulting orange oil was extracted with pentane (4 × 5 mL), and the combined extracts were filtered and concentrated to ∼5 mL to yield an orange, microcrystalline solid after standing at −40 °C overnight; the solid was washed with cold pentane and dried in vacuo. Yield: 0.200 g (0.29 mmol, 84%). ^{1}H NMR (C_6D_6, 20 °C): δ 1.69 [vt, N = 6.7 Hz, 6H, PC*H*$_3$(^{t}Bu)$_2$], 1.09 [vt, N = 13.8 Hz, 18H, PMe(C(C*H*$_3)_3)_2$], 1.06 [vt, N = 13.8 Hz, 18H, PMe(C(C*H*$_3)_3)_2$], 0.76 (td, J_{PH} = 26.0 Hz, J_{HH} = 7.2 Hz, 1H, Os*H*), −12.77 (td, J_{PH} = 15.4 Hz, J_{HH} = 7.2 Hz, 1H, Os*H*). ^{31}P{^{1}H} NMR (C_6D_6, 20 °C): δ 39.3 (s). ^{19}F NMR (C_6D_6, 20 °C): δ −79.1 (s). IR (C_6H_6): 1754 cm^{-1} (ν_{NO}).

OsH(D)$_2$(NO)L$_2$ (L = P^{i}Pr$_3$, P^{t}Bu$_2$Me). These isotopomers were generated by oxidative addition of D_2 to transient {$OsH(NO)L_2$}.[62] In a typical procedure, *cis*,*trans*-$OsH_2(OTf)(NO)L_2$ and at least 1.5 equiv of NpLi were placed in an NMR tube fitted with a Teflon stopcock (Young tube), C_6D_6 (0.6 mL) was vacuum transferred onto the solids, and the solid mixture was pressurized to 1 atm with D_2 at $T \approx -20$ °C. The mixture was vigorously shaken as it was thawing. ^{1}H NMR data recorded within 10 min showed a statistical 2:1 mixture of Os(D$_M$)(H$_A$D$_A$)(NO)L$_2$ and Os(H$_M$)(D$_A$)$_2$(NO)L$_2$, contaminated with variable amounts of $Os(H)_2D(NO)L_2$ and $Os(H)_3(NO)L_2$ (<10 mol %), as the only Os-containing products. The solutions were either redissolved in d_8-PhMe for NMR measurements or recrystallized from h_4-MeOH without any significant loss of D, if acidic impurities were rigorously excluded. Representative hydride signal shifts in **2b** on deuteration, relative to those in the all-protio case ($H_AH_AH_M$), recorded on a mixture of all possible isotopomers in C_6D_6 at 20 °C are as follows: $\Delta\delta$(H$_M$) (ppb) −45.5 ($H_AD_AH_M$), −93.0 ($D_AD_AH_M$); $\Delta\delta$(H$_A$) (ppb) −34.0 ($H_AH_AD_M$), +71.0 ($H_AD_AH_M$), +37.0 ($H_AD_AD_M$).

Low-Temperature Reaction of {OsH(NO)(P^{i}Pr$_3$)$_2$} with D$_2$. *cis*,*trans*-$OsH_2(OTf)(NO)(P^iPr_3)_2$ and ∼4 equiv of NpLi, both ground into fine powders, were placed in a 5-mm NMR tube annealed to a short manifold, which was capped with a Teflon valve, leading directly to the outlet of a 5-mL flask, which was also capped with a Teflon valve and from which d_8-PhMe was vacuum transferred onto the solids at −198 °C. The mixture was thawed at −40 °C, pressurized to 500 Torr with D_2, and frozen, and the NMR tube was sealed. The mixture was shaken in a −40 °C bath until the Os reagent had completely dissolved/reacted, cooled to −78 °C, and promptly transferred into the NMR probe, which was pre-cooled to −40 °C. ^{1}H NMR at this temperature revealed a H_A:H_M signal-intensity ratio of >4.2:1, which gradually decreased to 2:1 as the temperature was raised to 20 °C.

OsHDCl(NO)(P^{i}Pr$_3$)$_2$. $OsH(D)_2(NO)(P^iPr_3)_2$, generated as above, was dissolved in $CDCl_3$ in a Young tube for 2 h at RT, quantitatively yielding a 1:1:1 mixture of the HD, DH, and DD isotopomers, which was subsequently redissolved in d_8-PhMe for NMR measurements.

Os(D)$_3$(NO)(P^{i}Pr$_3$)$_2$. A solution of **2a** and 1 equiv of [Et_3NH][BF_4] was stirred in d_4-MeOH at RT for 30 h in a Young tube, after which time ^{1}H NMR showed >97 mol % deuteration of the hydride sites, and then brought to dryness. The solids were extracted with pentane, the solution was decanted off, and the pentane solubles were redissolved in heptane for IR measurements.

Ru(H)$_3$(NO)L$_2$ [L = P^{i}Pr$_3$ (1a), P^{t}Bu$_2$Me (1b)][40] and Ru(D)$_3$(NO)(P^{t}Bu$_2$Me)$_2$ (1b-*d*$_3$). A solution of *trans*-$RuMe(NO)L_2$ in d_{10}-Et_2O (for NMR measurements) or heptane (for IR measurements) in a Young tube was freeze−pump−thaw degassed three times and pressurized to 1 atm with H_2 (NMR) or D_2 (IR), quantitatively forming the corresponding trihydrides and methane within minutes.

RuH(D)$_2$(NO)(P^{i}Pr$_3$)$_2$. A solution of *trans*-$RuMe(NO)(P^iPr_3)_2$ in d_{10}-Et_2O in a Young tube was freeze−pump−thaw degassed three times and subjected to <1 equiv of H_2. The mixture was allowed to equilibrate at RT for several hours, until the **1a** hydride signals were barely visible by ^{1}H NMR at −70 °C. The solution was cooled to −100 °C, pressurized to 1 atm with D_2, and transferred in the NMR probe precooled to −95 °C. As with the Os analogues, ^{1}H NMR showed ∼5 mol % contamination with the $(H)_2D$ and $(H)_3$ isotopomers.

RuH(NO)(P^{t}Bu$_2$Me)$_2$[40] and RuD(NO)(P^{t}Bu$_2$Me)$_2$. Solutions of **1b** and **1b-*d*$_3$**, generated as above in heptane, were brought to dryness, redissolved in heptane, and brought to dryness again several times to ensure maximum loss of H_2 or D_2. IR spectra of the complexes generated in this way, recorded within an hour, showed residual 15−20 mol % of **1b** and **1b-*d*$_3$** along with trace decomposition. Addition of substoichiometric H_2 to $RuMe(NO)(P^iPr_3)_2$ as above was used to generate the complexes for NMR measurements.

Studies of Reactivity of 2a−c. All reactions were carried out on the NMR scale in Young tubes and monitored by ^{1}H and ^{31}P NMR. In the case of attempted exchange with D_2, the hydride signals of **2c** showed constant integration against the phosphine aryl resonances for 24 h at RT in C_6D_6, whereas partly deuterated analogues of **2a**,**b** generated otherwise can be observed separately (not exchange averaged) and were absent in the D_2 reactions.

***T*$_1$ Measurements and Derivation of r_{HH}.** All T_1 measurements were performed at 300 MHz (^{1}H) using standard inversion−recovery Varian software. Full details are provided in the Supporting Information. In brief, T_{1min} values were located with multiple points around T°C(T_{1min}), were corrected for intramolecular hydride site exchange in **1b**, and were treated with appropriate error limits (≥5%) that were assumed by consideration of several factors. The dominance of an intramolecular ^{1}H−^{1}H dipolar relaxation mechanism was demonstrated for **2a** by comparison of experimental R* values to those evaluated from the crystal structure. The effects of significantly anisotropic tumbling were considered, and upper estimates on r_{HH} values were derived.

^{1}H NMR Spectral Simulation. Experimental exchange-broadened line shapes were iteratively fit using the gNMR[92] program, with line widths in the absence of exchange fixed at the lowest measured values. For intramolecular exchange in **1b**, J_{HH} values obtained at temperatures from −95 to −60 °C were extrapolated to higher temperatures according to an exponential law[93] (Figure S1, Supporting Information) and kept constant during simulations. The activation parameters assumed 10% errors in k_{HH} and 1 °C errors in T°C. Variations in the line width with temperature, as measured for Os analogue **2b**, gave negligible variations in k_{HH}.

Computational Details. All calculations were performed with the Gaussian 94[94] and Gaussian 98[95] suites of programs, using hybrid density functional method B3LYP,[96] with LANL2DZ[97−99], called BS I, a valence double-ζ basis set with relativistic effective core potentials for the Os[98] and P[99] centers, and BS II, an extension of BS I in which all H, N, and O atoms are described with a 6-31G[100] basis set, supplemented with polarization functions[101] for (Os)H, N, and O, and polarization functions are used for P.[102] All PH_3 structures were fully optimized with standard convergence criteria without symmetry constraints and converged to essentially C_s or C_{2v} symmetry. All PMe_3 structures were thus optimized with C_s symmetry. All structures presented in Figures 5 and 6 were confirmed to be true minima or transition states via frequency analysis,[95] which was also used to calculate zero-point energies (ZPE) without scaling. For **TS(B)**-[RuNO], C_s symmetry was imposed for frequency calculations, because C_1-optimized geometry, although marginally different, invariably had a second imaginary frequency of ∼11 cm^{-1} that corresponded to the breaking of the effective C_s symmetry by the asymmetric rotation of the PH_3 groups. For all transition states, motion corresponding to the imaginary frequency was visually checked, and most structures were additionally optimized to the minima they connected after correspondingly perturbing the TS geometry. For H_2 loss from the **TS(B)**-[RuCO]$^-$, **TS(B)**-[OsNO], and **C**-[RuNO] structures, such optimizations led to end-on bonded η^1-H_2 complexes with marginal binding energies that were unbound (or nearly so with ZPE) and had no physical significance. MOs in Figure 7 were plotted with Molden.[103] Cartesian coordinates of all structures discussed in the text are provided in the Supporting Information.

Acknowledgment. This work was supported by the NSF and by a graduate fellowship to D.V.Y. D.V.Y. gratefully acknowledges stimulating discussions with Professors Odile Eisenstein and Ernest R. Davidson.

Supporting Information Available: A plot showing an exponential temperature dependence of J_{HH} in **1b**, full details of T_1 measurements and the derivation of r_{HH}, full X-ray structural information on **2a**, and Cartesian coordinates of all optimized structures. This material is available free of charge via the Internet at http://pubs.acs.org.

IC991452J

(92) Budzelaar, P. H. M. *gNMR*, version 3.6.5; IvorySoft: Englewood, CO, 1995. (Published by Cherwell Scientific Publishing Limited, Oxford, U.K.)
(93) Limbach, H.-H.; Ulrich, S.; Gründemann, S.; Buntkowsky, G.; Sabo-Etienne, S.; Chaudret, B.; Kubas, G. J.; Eckert, J. *J. Am. Chem. Soc.* **1998**, *120*, 7929.
(94) Frisch, M. J.; Trucks, G. W.; Schlegel, H. B.; Gill, P. M. W.; Johnson, B. G.; Robb, M. A.; Cheeseman, J. R.; Keith, T.; Petersson, G. A.; Montgomery, J. A.; Raghavachari, K.; Al-Laham, M. A.; Zakrzewski, V. G.; Ortiz, J. V.; Foresman, J. B.; Cioslowski, J.; Stefanov, B. B.; Nanayakkara, A.; Challacombe, M.; Peng, C. Y.; Ayala, P. Y.; Chen, W.; Wong, M. W.; Andres, J. L.; Replogle, E. S.; Gomperts, R.; Martin, R. L.; Fox, D. J.; Binkley, J. S.; Defrees, D. J.; Baker, J.; Stewart, J. P.; Head-Gordon, M.; Gonzalez, C.; Pople, J. A. *Gaussian 94*, revision D.1; Gaussian, Inc.: Pittsburgh, PA, 1995.
(95) Frisch, M. J.; Trucks, G. W.; Schlegel, H. B.; Scuseria, G. E.; Robb, M. A.; Cheeseman, J. R.; Zakrzewski, V. G.; Montgomery, J. A., Jr.; Stratmann, R. E.; Burant, J. C.; Dapprich, S.; Millam, J. M.; Daniels, A. D.; Kudin, K. N.; Strain, M. C.; Farkas, O.; Tomasi, J.; Barone, V.; Cossi, M.; Cammi, R.; Mennucci, B.; Pomelli, C.; Adamo, C.; Clifford, S.; Ochterski, J.; Petersson, G. A.; Ayala, P. Y.; Cui, Q.; Morokuma, K.; Malick, D. K.; Rabuck, A. D.; Raghavachari, K.; Foresman, J. B.; Cioslowski, J.; Ortiz, J. V.; Stefanov, B. B.; Liu, G.; Liashenko, A.; Piskorz, P.; Komaromi, I.; Gomperts, R.; Martin, R. L.; Fox, D. J.; Keith, T.; Al-Laham, M. A.; Peng, C. Y.; Nanayakkara, A.; Gonzalez, C.; Challacombe, M.; Gill, P. M. W.; Johnson, B.; Chen, W.; Wong, M. W.; Andres, J. L.; Gonzalez, C.; Head-Gordon, M.; Replogle, E. S.; Pople, J. A. *Gaussian 98*, revision A.6; Gaussian, Inc.: Pittsburgh, PA, 1998.
(96) Becke, A. D. *J. Chem. Phys.* **1993**, *98*, 5648. Lee, C.; Yang, W.; Parr, R. G. *Phys. Rev. B* **1988**, *37*, 785. Stephens, P. J.; Devlin, F. J.; Chabalowski, C. F.; Frisch, M. J. *J. Phys. Chem.* **1994**, *98*, 11623.
(97) Frisch, M. J.; Trucks, G. W.; Schlegel, H. B.; Gill, P. M. W.; Johnson, B. G.; Wong, M. W.; Foresman, J. B.; Robb, M. A.; Head-Gorden, M.; Replogle, E. S.; Gomperts, R.; Andres, J. L.; Raghavachari, K.; Binkley, J. S.; Gonzalez, C.; Martin, R. L.; Fox, D. J.; Defrees, D. J.; Baker, J.; Stewart, J. J. P.; Pople, J. A. *Gaussian 92/DFT*; Gaussian, Inc.: Pittsburgh, PA, 1993.
(98) Hay, P. J.; Wadt, W. R. *J. Chem. Phys.* **1985**, *82*, 299.
(99) Wadt, W. R.; Hay, P. J. *J. Chem. Phys.* **1985**, *82*, 284.
(100) Hehre, W. J.; Ditchfield, R.; Pople, J. A. *J. Chem. Phys.* **1972**, *56*, 2257.
(101) Hariharan, P. C.; Pople, J. A. *Theor. Chim. Acta* **1973**, *28*, 213.
(102) Höllwarth, A.; Böhme, M.; Dapprich, S.; Ehlers, A. W.; Gobbi, A.; Jonas, V.; Köhler, K. F.; Stegmann, R.; Veldkamp, A.; Frenking, G. *Chem. Phys. Lett.* **1993**, *208*, 237.
(103) Schaftenaar, G. *Molden*, version 3.2.; CMBI: Nijmegen, The Netherlands, 1991.